89p.

HYDRONAUTICS, incorporated
research in hydrodynamics

Research, consulting, and advanced engineering in the fields of NAVAL and INDUSTRIAL HYDRODYNAMICS. Offices and Laboratory in the Washington, D. C., area: Pindell School Road, Howard County, Laurel, Md.

HYDRONAUTICS, Incorporated

TECHNICAL REPORT 235-1

CAVITATION DAMAGE IN LIQUID SODIUM

By

H. S. Preiser, A. Thiruvengadam,

and

C. E. Couchman, III

Prepared for
National Aeronautics and Space Administration
April 1, 1964
Contract NASr-105

Technical Management
NASA Lewis Research Center
Nuclear Power Technology Branch
James P. Couch

HYDRONAUTICS, Incorporated
Pindell School Road
Laurel, Maryland

NOTICE

LIST OF FIGURES

TABLE OF CONTENTS

ABSTRACT

26470

For the past two years HYDRONAUTICS, Incorporated has been engaged in work on cavitation damage in liquid sodium. Suitable test facilities and techniques to conduct these investigations in high temperature liquid metals have been developed in this program. The considerations that governed the selection and development of a suitable laboratory facility are discussed. The operational experience gained from using such a facility are presented. Based on this experience, an improved facility has been developed for testing refractory metals at temperatures up to 1500°F in liquid sodium. The high frequency fatigue testing techniques developed for these investigations are described. Experiments designed to standardize magnetostriction test parameters are included along with a description of the components of the magnetostriction apparatus. An analysis was made to correlate the cavitation damage resistance of several metals in liquid sodium with their mechanical properties. The intensity of cavitation damage in impure liquid sodium at 400°F was estimated from these data. Future work in the areas of cavitation damage resistance of refractory metals is also outlined.

author

INTRODUCTION

Research on cavitation damage in liquid alkali metals at high temperatures is motivated by the need for development of light weight auxiliary power generating equipment for future space vehicles in which liquid alkali metals are to be used as the thermodynamic working fluid. HYDRONAUTICS, Incorporated has been engaged in intensive investigations for the past two years with the ultimate goal of developing meaningful design parameters for the determination of resistance of materials to cavitation damage in liquid metals. This is the final report summarizing the conclusions resulting from the investigations sponsored by National Aeronautics and Space Administration under Contract NASr-105.

Recent investigations at HYDRONAUTICS, Incorporated with a magnetostrictive oscillator using distilled water and NaCl solutions have produced relationships of the material response to the power output parameters. These relationships also have been determined for the case of five metals (pure iron, 201 nickel, 316 stainless steel, 600 inconel and 100A titanium) in oxygen saturated liquid sodium at 400°F. For one metal, 100A titanium, these experiments were extended to 1000°F.

EXPERIMENTAL FACILITIES AND TECHNIQUES

Criteria for the Selection of the Type of Facility

There are several types of test facilities used for cavitation damage research. The choice of a suitable facility for alkali metal operation is governed by the following criteria.

1. The cavitation device should produce sufficient intensity to permit relatively short testing times.

2. The cavitation device should be capable of simple operation, precise control, reliable calibration, and yield frequent and reproducible data for analyses without serious interruption or shut down.

3. The cavitation device should be compact and suitable for operation in an inert atmosphere to prevent contamination of the liquid alkali metal.

4. The liquid metal volume in the system should be kept to a minimum to enhance ease and safety of storage, transfer, purification and heating.

5. The entire facility should be economical to construct and operate, and require minimum floor space.

6. The facility should be versatile for conducting experiments related to cavitation damage, such as fatigue and stress corrosion studies.

Among the three types of devices (namely magnetostriction, flow venturi, and rotating disk) that are generally used for cavitation damage research, the magnetostriction device appears to have the best chance of satisfying the above criteria. Intensive efforts have gone into the development of a suitable test facility around the magnetostriction apparatus. The apparatus has been in operation for over 1-1/2 years and based on this experience, a new improved facility has been constructed.

There have been parallel developments elsewhere to use the other two types of facilities, namely, the flow device reported in Reference (1) and the rotating disk device reported in Reference (2). An earlier attempt to use the magnetostriction apparatus in liquid metal studies was only partially successful (3).

Magnetostriction Device for Cavitation Damage Research

Magnetostriction devices for laboratory studies of cavitation damage phenomena have been used by many investigators in the past (4). In recent years many improvements have been made on these devices such as simplification of circuits, reduction of power consumption, increase in efficiency and ease of operation. Mason (5) introduced the idea of an exponential horn coupled to a transducer which performed the function of a velocity transformer. This idea was utilized at California Institute of Technology (6) to attain substantial linear vibratory motion at relatively high amplitudes (2×10^{-3} inches) from a modest power input of 200 watts. Further magnification of amplitude from the same power source is possible by stepped cylindrical horns in lieu of the exponential types (7). Extensive work has been accomplished for obtaining reproducible and reliable cavitation damage data by magnetostriction testing. Part of these data were obtained under Office of Naval Research Contract No. Nonr 3755(00) FBM NR 062-293, and are reported in the Appendix 1 for the sake of completeness (see also Reference (8)).

In view of the simplicity of operation, ease of control of the test parameters of interest, small size and weight of the equipment, inexpensive preparation, weighing and examination of

the specimens, it was decided to adapt the magnetostriction device to a cavitation damage test facility for high temperature liquid alkali metals. Essentially, a vacuum dry box enclosure was chosen to contain an inert atmosphere around the magnetostriction device which vibrated a specimen in a heated retort of liquid alkali metal. This arrangement overcame many operational problems which no doubt plagued the earlier investigations previously mentioned (3).

Design Criteria for the Magnetostriction Test Facility

The following design criteria are required for an acceptable facility for testing refractory materials in liquid alkali metals at high temperatures.

1. Means for providing and maintaining a clean, controlled inert environment in contact with the liquid alkali metal. This environment should be essentially free of oxygen, hydrogen, moisture and carbon containing materials;

2. Means for storing, purifying, charging, transferring, sampling and discarding liquid alkali metals used in the test, in a safe, efficient manner;

3. Means for remotely operating and controlling the magnetostriction device such as accurate positioning of the specimen in the test liquid; varying amplitude and frequency; frequently removing specimens for examination and weighing; conducting related fatigue tests at corresponding frequencies and suspending static stress corrosion coupons;

4. Means for varying and controlling the temperature of the liquid metal in the test retort and throughout other parts of the liquid metals loop;

5. Means for varying the pressure above the test liquid and preventing escape of liquid metal vapors from test retort;

6. Means for cooling work areas, critical seals and operating components to safe temperatures;

7. Means for miscellaneous operations such as frequent access to work areas; calibration of magnetostriction device in place; bake-out of specimens prior to testing; insurance of safe operation, adequate lighting and electrical and instrument services.

The Initial Facility

With the above design criteria as a guide, a limited, low cost dry box facility was fabricated to gain operational experience and preliminary cavitation damage data in liquid sodium. The most economical methods were chosen to meet the design criteria, and in most cases, these methods fell short of complete attainment.

A simple, non-structural purge type of dry box was constructed in which air was removed from the enclosure by displacement with commercial-grade cover-gas. The gas was dried to -80°F dew-point in a commercially available dessicant dryer. No instrumentation was provided to measure the moisture or oxygen content of the inert atmosphere in the dry box. The general arrangement of the dry box is shown in Figure 1.

1. GAS CONTROL APPARATUS
2. DRY BOX
3. AIR LOCK
4. GLOVE PORTS
5. FURNACE AND CONTROL
6. POWER SUPPLY AND CONTROLS FOR MAGNETOSTRICTION APPARATUS

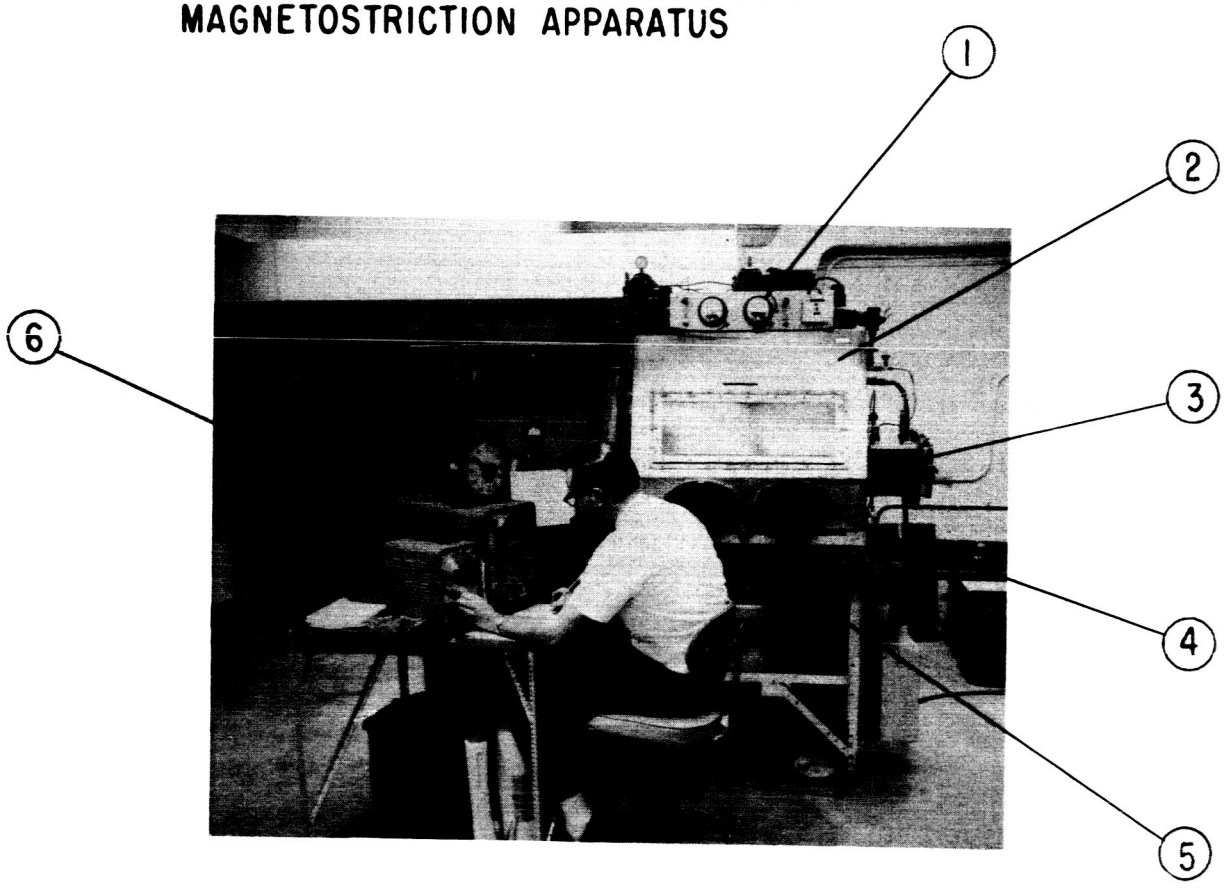

FIGURE 1. GENERAL ARRANGEMENT OF INITIAL CAVITATION DAMAGE FACILITY

No provisions were made to purify the sodium before filling the test retort. Dry, one pound bricks of regular grade sodium were brought into the dry box through a purge type of air lock and melted in the retort. All surface oxides were skimmed off the top by means of a sieve type ladle. A cold trap stub was provided in the bottom of the retort to precipitate oxides at 250°F. A drain valve at the bottom of the cold trap facilitated discarding of the spent sodium as shown in Figure 2.

The magnetostriction apparatus was mounted on a travelling crosshead which was moved up and down on vertical guide rails by means of a motorized lead screw. The elevating motor was mounted outside the dry box and the driving lead screw was sealed in a packed gland. All electrical controls for the magnetostriction apparatus were located outside the box. Figure 3 is a block diagram of the essential components of the magnetostriction apparatus. It consists of an audio oscillator, a 200 watt amplifier and power supply, a magnetostriction transducer, a velocity transformer, a displacement pick-up coil, an oscilloscope and a test specimen. A brief description of the function and design of each of these components is given in Appendix II.

A retort furnace was provided with an automatic temperature controller to maintain liquid metal temperature within ± 15°F.

Cooling of the magnetostriction apparatus and retort head was accomplished by means of an internal fan blowing argon gas over a set of water cooled coils (seamless stainless steel).

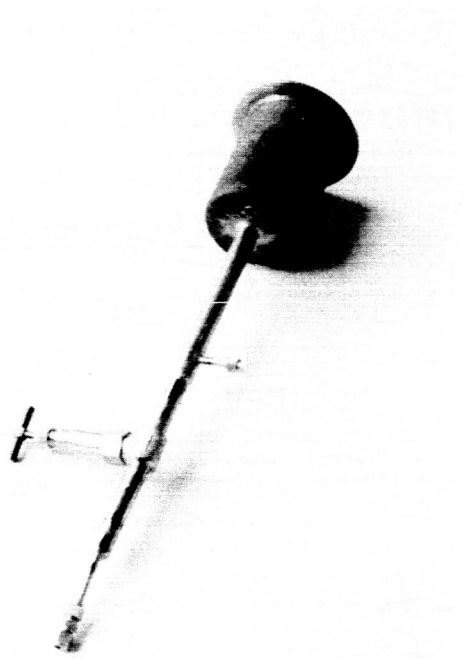

FIGURE 2. COLD TRAP ASSEMBLY FOR INITIAL FACILITY

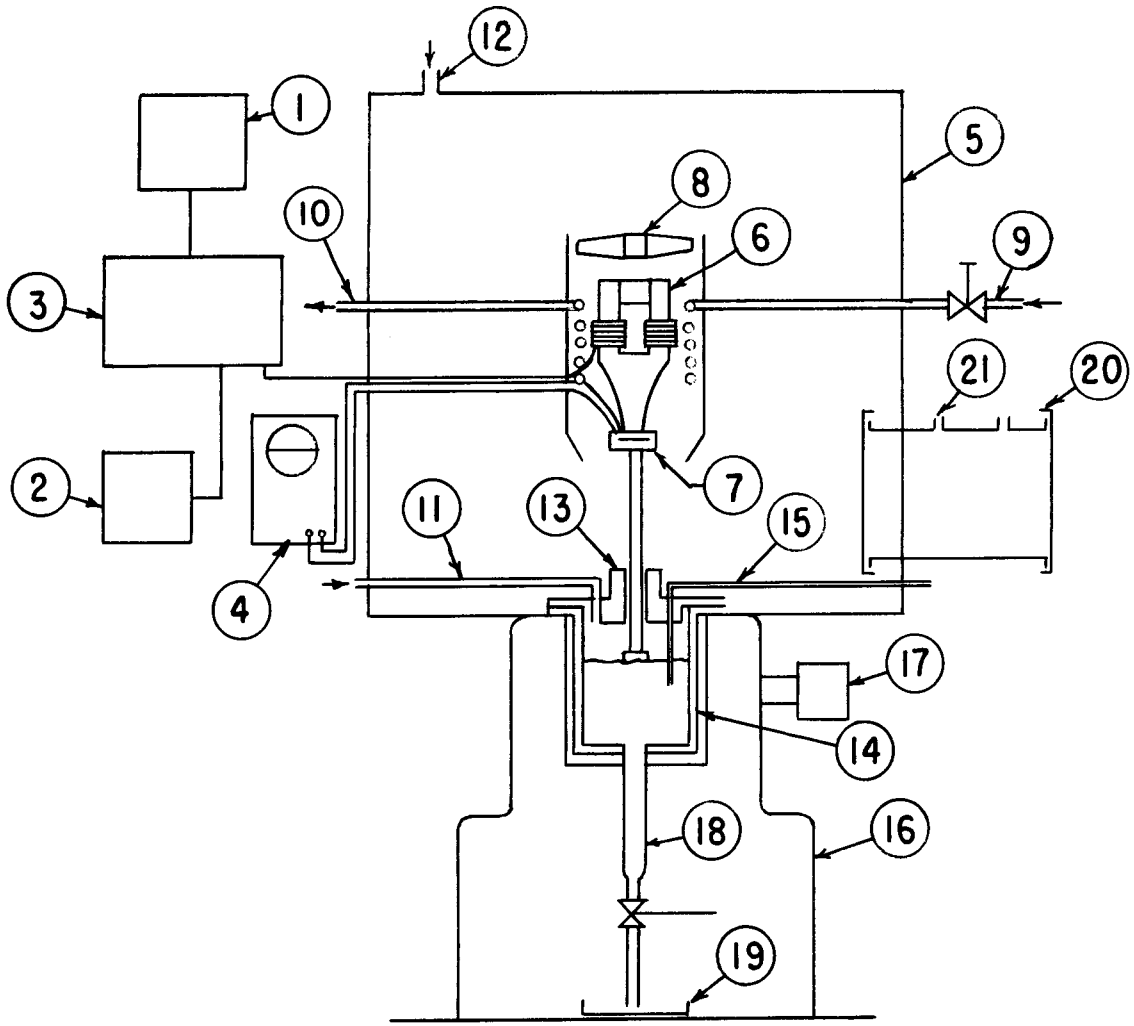

1. POWER SUPPLY
2. AUDIO OSCILLATOR
3. 200 WATT AMPLIFIER
4. OSCILLOSCOPE
5. DRY BOX
6. TRANSDUCER STACK
7. PICK-UP COIL
8. FAN
9. COOLING WATER IN
10. COOLING WATER OUT
11. DRY ARGON FOR RETORT
12. DRY ARGON FOR BOX
13. RETORT HEAD
14. RETORT
15. INDICATING THERMOCOUPLE
16. RETORT FURNACE
17. PYROMETER CONTROL FOR FURNACE
18. SODIUM COLD TRAP
19. SODIUM DRAIN PAN
20. GAS LOCK
21. DRY ARGON FOR GAS LOCK

FIGURE 3. BLOCK DIAGRAM OF MAGNETOSTRICTION APPARATUS FOR INITIAL FACILITY

The magnetostriction horn was isolated electrically from the dry box to permit the specimen to close an indicating circuit upon contact with the sodium. There was no way in which calibration of the apparatus could be made in place. This proved to be very cumbersome.

Lighting was furnished by two 60 watt bulbs which were wired internally. Thermocouple stuffing glands were used for all electrical feed-thru connections. A low pressure alarm was provided to indicate when cover gas supply was nearly exhausted.

It turned out that the major difficulty experienced with the dry box was leakage around seals, particularly, at the air lock and retort. This required the use of large amounts of argon at gage pressures of 2 to 3 inches of water to maintain the inert atmosphere. Diffusion of the oxygen through these leaky seals contributed largely to the contamination problem with the sodium. Also, inadequate sealing of the magnetostriction rod entering the retort resulted in substantial sodium vapor condensing inside the dry box which fogged the viewing window and caused occasional electrical shorts.

In spite of these problems, the preliminary data obtained were encouraging enough to promote construction of an improved facility. The data presented in the latter section of the report has the following limitations which are expected to be eliminated in the new cavitation test facility:

(a) Inert atmosphere could not be carefully controlled. Displacement with cover gas was inadequate to maintain an atmosphere with total contamination of O_2, N_2 and H_2O of less than 5 ppm.

(b) The oxide levels in sodium can be assumed to be saturated at the test temperature. In several cases these oxide levels were considerably over 50 ppm.

(c) Inadequate cooling and gasket arrangements prevented temperature runs above 1000°F.

(d) Infrequent changing of sodium in retort probably resulted in a certain amount of ion contamination from the testing of several different specimen materials.

(e) Specimen immersion control was difficult due to formation of a surface deposit on the sodium which prevented accurate determination of the liquid level.

Features of the New Test Facility

Based on the experience gained with the initial facility and the further need for critical control of the environment for refractory metal studies, a new facility was designed which incorporated many improvements and modifications. Tight specification control was exercised over fabrication and performance requirements. The new facility was designed to handle liquid sodium up to temperatures of 1500°F and pressures up to 5 psig.

The test facility consists of the following equipment categories:

1. Inert Environment - The components associated with providing an inert environment are the dry box, retort assembly, vacuum system and the cover gas system with related instrumentation.

(a) Dry box - A vacuum chamber was designed to be evacuated to a minimum pressure of 2.5 microns of mercury prior to back flushing with pure argon cover gas. The chamber can withstand internal gas pressures up to 5 psig including sudden surges from full vacuum to full pressure. The internal areas of the dry box are free of lubricants, refractory and carbon containing materials except for minor packings and seals. A standard sloped-front dry box 48" L x 31" D x 28" H, was modified with special access openings for an air lock, specimen lock, tubular housing for the magnetostriction device, rear door, view ports, lighting ports, utilities and instrument connections. A false bottom is fabricated in the box for cooling purposes. All control consoles for essential systems are incorporated into the external support frame. The entire facility is mounted on a movable dolly. The general arrangement is shown in Figure 4.

The dry box is constructed of 304 stainless steel, externally braced as necessary. All internal welds are full filet welds ground back to a number four satin finish. External metal joints are continuously welded after ascertaining leak tightness in conformance with highest quality vacuum practice.

(b) Retort Assembly - The bottom of the dry box is constructed with a special flange arrangement to permit a retort to be bolted in place by means of a metallic O-ring seal. The water cooled false bottom is arranged so as not to interfere with the retort connection. The retort will be described in more detail under the section on Sodium Handling below.

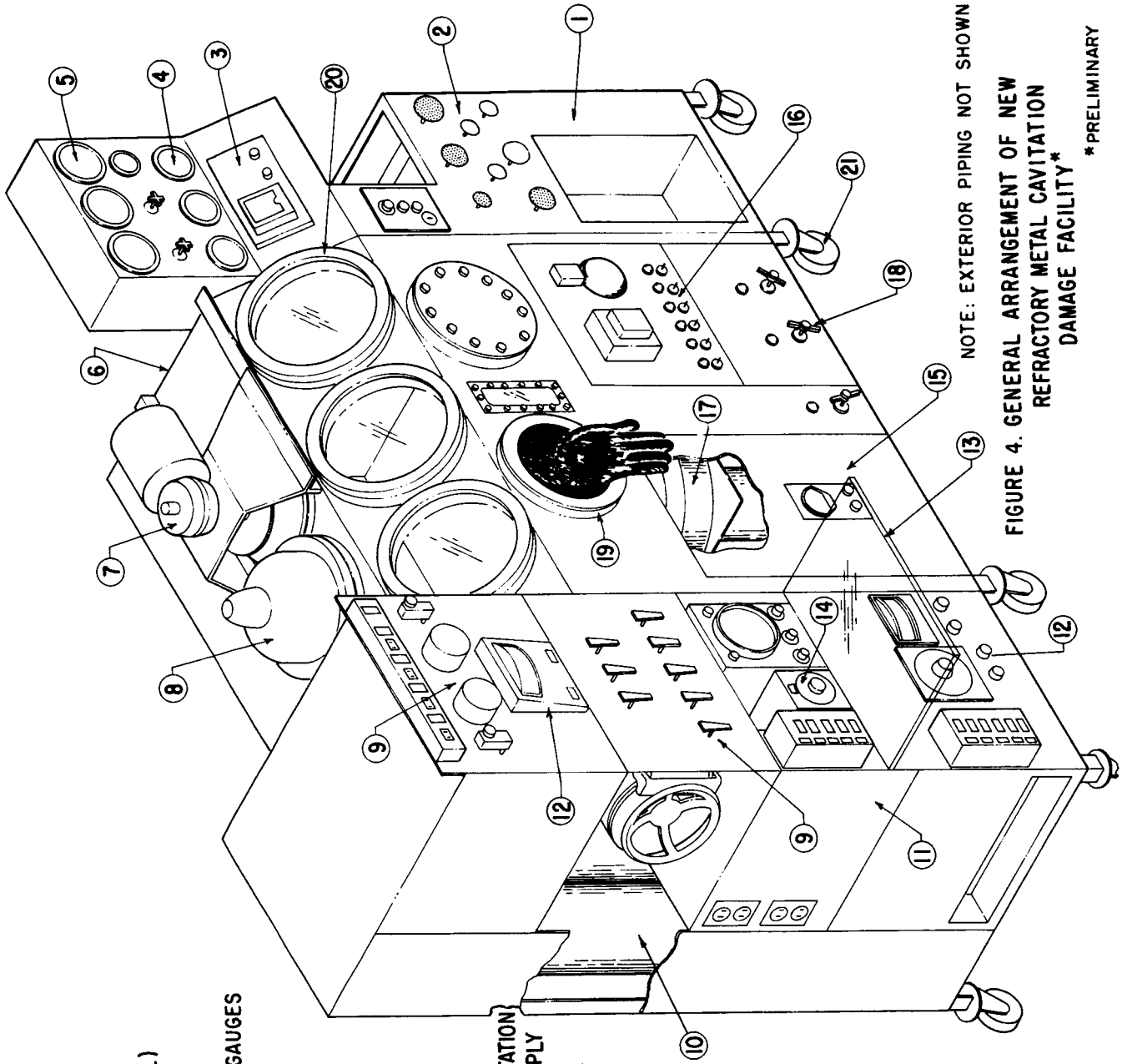

NOTE: EXTERIOR PIPING NOT SHOWN

FIGURE 4. GENERAL ARRANGEMENT OF NEW REFRACTORY METAL CAVITATION DAMAGE FACILITY*

*PRELIMINARY

(c) Vacuum System - To achieve the vacuum requirements in the dry box set forth above, a 15 cfm mechanical pump was selected. Pump down after initial outgassing is accomplished in about one hour. The pump is isolated and shock mounted to prevent transmission of mechanical vibrations to the dry box or its supports. The vacuum manifolds and piping are fabricated from hard drawn copper, adequately sized for efficient pump down. All valves in the system are high vacuum sweat solder types with metallic bellows. The system was thoroughly cleaned of all oil and visible oxides before assembly and leak checked with a helium mass spectrometer after assembly.

Figure 5 shows a schematic piping and instrument arrangement of the vacuum system. A keyed master switch is provided to control the pump switch to prevent accidental starting of the vacuum pump. The cooling water pump switch is also inter-locked with the vacuum pump to prevent excessive pressure in the false bottom of the dry box which could put undue strain on critical welds at the seams.

(d) Cover Gas System - An inert atmosphere of pure argon surrounds all components which are in contact with or have access to the liquid sodium commercially available, high purity argon, with total moisture, oxygen and nitrogen of less than 5 ppm, is used. The cover gas is introduced into the dry box (back flushed) after evacuation of air. Initially, alternate vacuum purging and back flushing with argon is repeated until oxygen and moisture content in the dry box are below 5 ppm total.

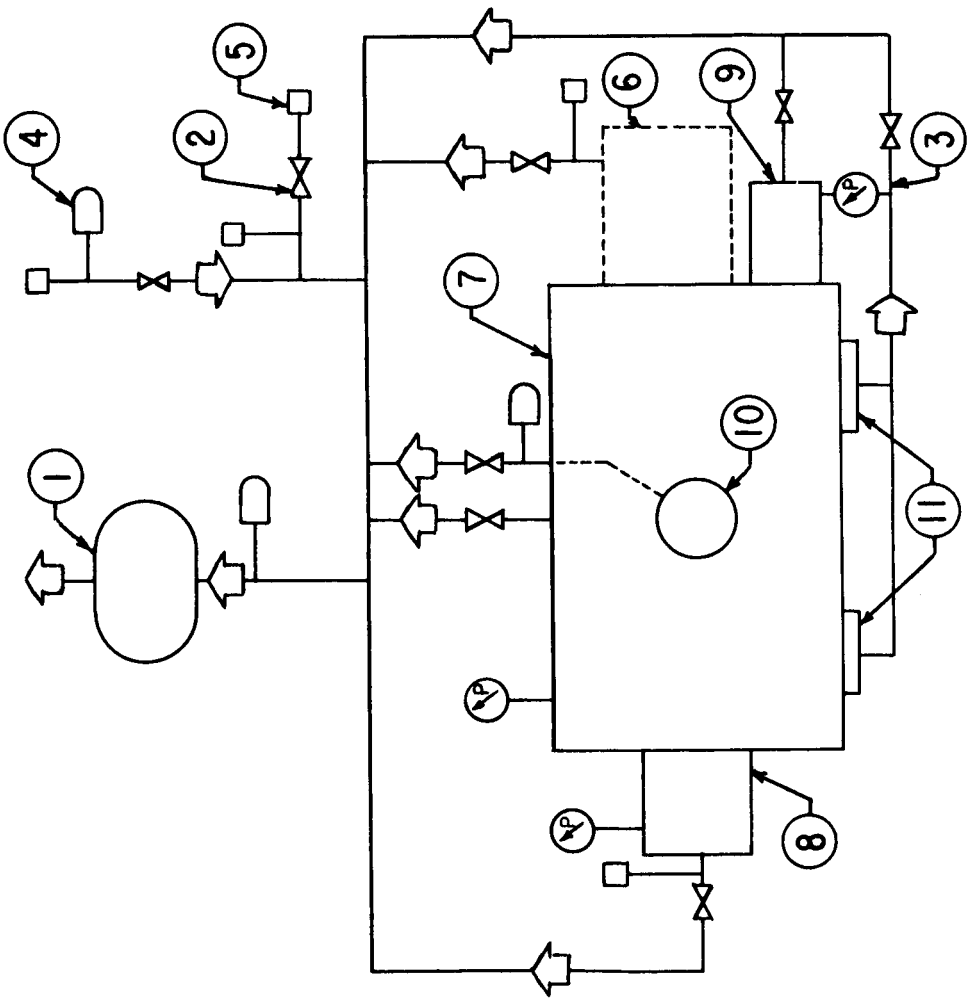

FIGURE 5. SCHEMATIC VACUUM SYSTEM FOR NEW FACILITY

In addition to providing an inert atmosphere over the sodium, cover gas pressure is also used to transport liquid sodium throughout the different parts of the sodium handling system, which is described later. A schematic diagram, Figure 6, shows the layout of the cover gas system. A pressure alarm switch indicates when the gas flask is nearly empty so that a replacement can be switched on the line without interrupting operations. Another safety feature provided is a solenoid operated valve which shuts off the gas system while the vacuum pump is running.

As part of the cover gas system, (see Figure 7), monitoring stations are set up to measure oxygen and moisture in the cover gas on a periodic basis. An alarm will be incorporated into the system to warn the operator of high moisture or O_2 content in the cover gas.

2. Sodium Handling - The components associated with the liquid metals system are the retort assembly, storage, charging and drainage tanks, connecting loop, and related instrumentation.

(a) Retort Assembly - A standard 5 inch diameter, high nickel alloy pot for the furnace was modified to bolt to the bottom flange adapter of the dry box. The retort is fitted with a sodium fill and drain line and an overflow line to permit a constant level of liquid to be maintained. An externally mounted furnace surrounds the retort and an additional clamp-shell heater is fitted around the sodium piping leading into the retort. This is necessary to provide adequate heating capacity for high temperature tests. The furnace details will be described later. All

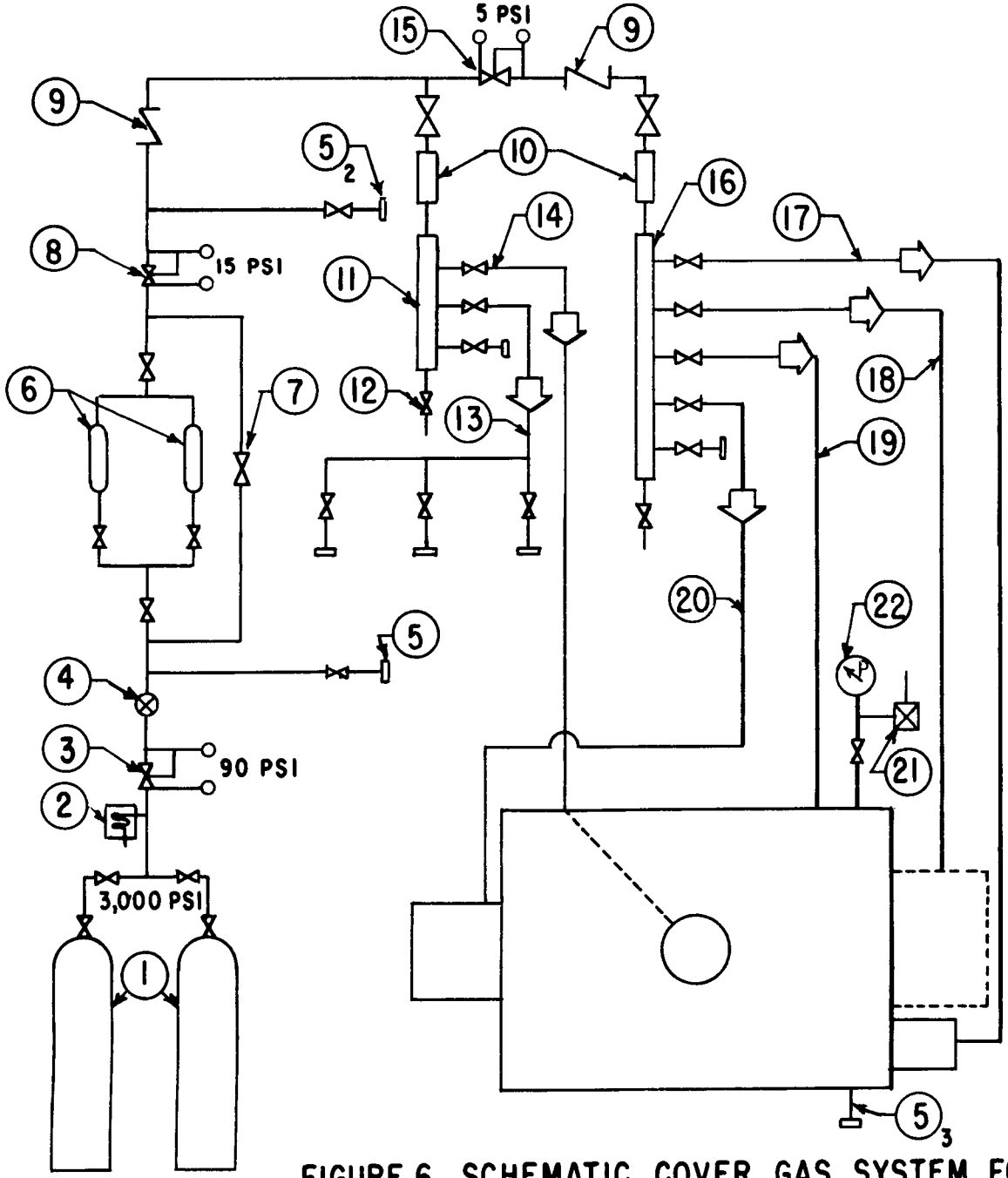

1. ARGON COVER GAS BOTTLES
2. LOW PRESSURE ALARM
3. REGULATOR (90 PSI)
4. SOLENOID VALVE
5. ANALYZING STATION
6. GAS DRYER
7. BY-PASS VALVE
8. REGULATOR (15 PSI)
9. CHECK VALVE
10. FLOW METERS
11. MANIFOLD (15 PSI)
12. BLEED LINE
13. SODIUM SYSTEM (GAS)
14. RETORT (GAS)
15. REGULATOR (5 PSI)
16. MANIFOLD (5 PSI)
17. SPECIMAN CHUTE (GAS)
18. VACUUM FURNACE (GAS)
19. DRY BOX (GAS)
20. AIR LOCK (GAS)
21. PURGE & RELIEF VALVE (5 PSI)
22. PRESSURE GAUGE (DRY BOX)

FIGURE 6. SCHEMATIC COVER GAS SYSTEM FOR NEW FACILITY

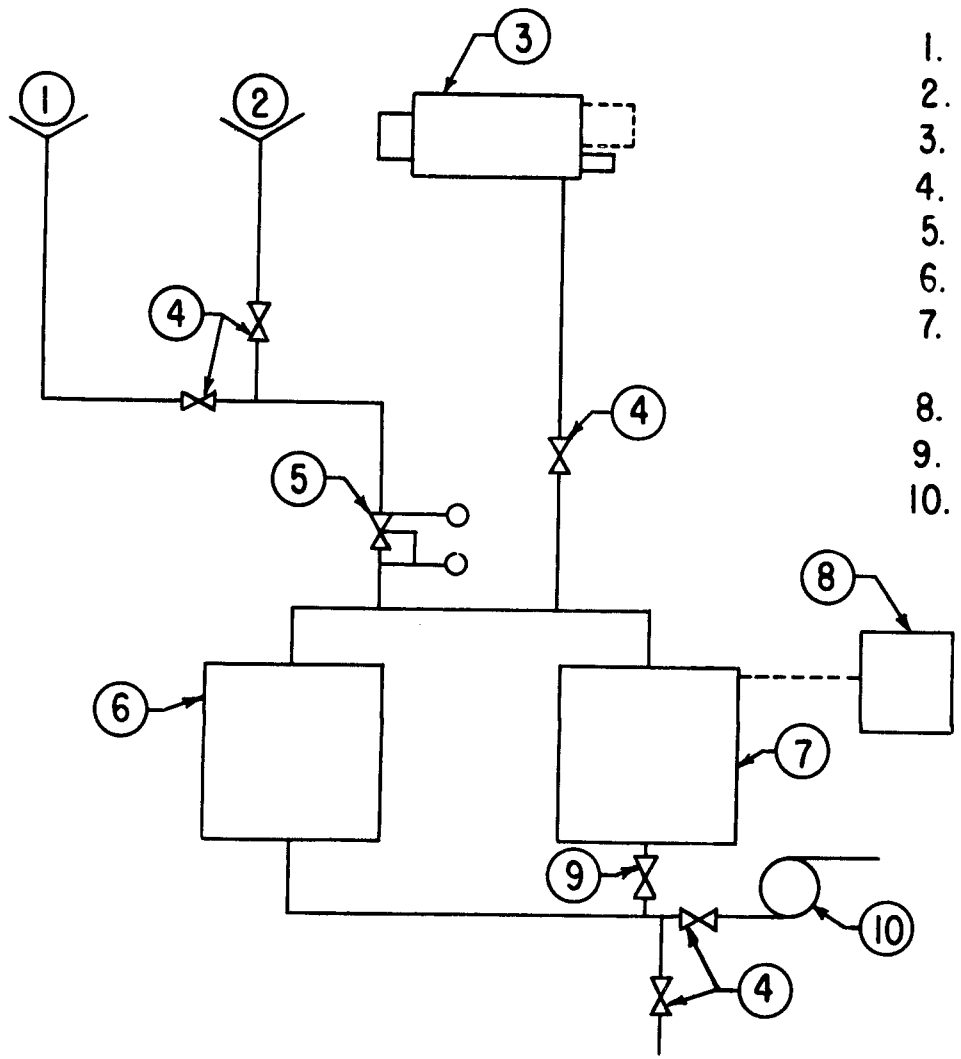

1. ANALYZING STATION NO.1
2. ANALYZING STATION NO.2
3. DRY BOX
4. TOGGLE VALVES
5. REGULATOR (5 PSI)
6. HYGROMETER (BECKMAN - NO.719)
7. OXYGEN INDICATOR (ANALYTIC SYSTEMS COMPANY - SERIES 300)
8. MV POTENTIOMETRIC RECORDER
9. NEEDLE VALVE
10. SAMPLE PUMP

FIGURE 7. SCHEMATIC GAS ANALYSIS SYSTEM FOR NEW FACILITY

piping and valves in contact with liquid sodium are fabricated from 316 stainless steel. Valves are bellows sealed and vacuum tight. The welds are of radiographic quality made by the inert gas shielded, tungsten-arc process intended for high temperature sodium service, and they conform to appropriate sections of ASME Unfired Pressure Vessel Code and liquid metal specifications. The details of the retort assembly are shown in Figure 8.

The retort head, which is bolted to a flange assembly inside the dry box, completely isolates the retort assembly from the dry box. This arrangement permits independent control of pressures in the retort for setting experimental conditions as well as for versatility in filling and draining without disturbing the main chamber environment. The retort head as shown in Figure 8 allows insertion of the specimen, mounted on the magnetostriction horn extension, into the sodium through a vapor tight telescopic seal. Thermocouples are positioned in the retort head at two levels to permit readout of the sodium level during filling and draining. The telescopic seal is fitted with a small band heater to permit melting of condensed sodium in the joint should this become necessary. Push-rod clean out probes have been provided in the gas and vacuum line entering the retort head to unplug the line from sodium condensate accumulations which may occur during operation.

(b) Storage, Charging and Drainage Tanks - In order to facilitate handling and purification of the sodium, reactor grade sodium is cold trapped commercially to 50 ppm oxide content and shipped in clean 30 gallon reinforced stainless steel drums.

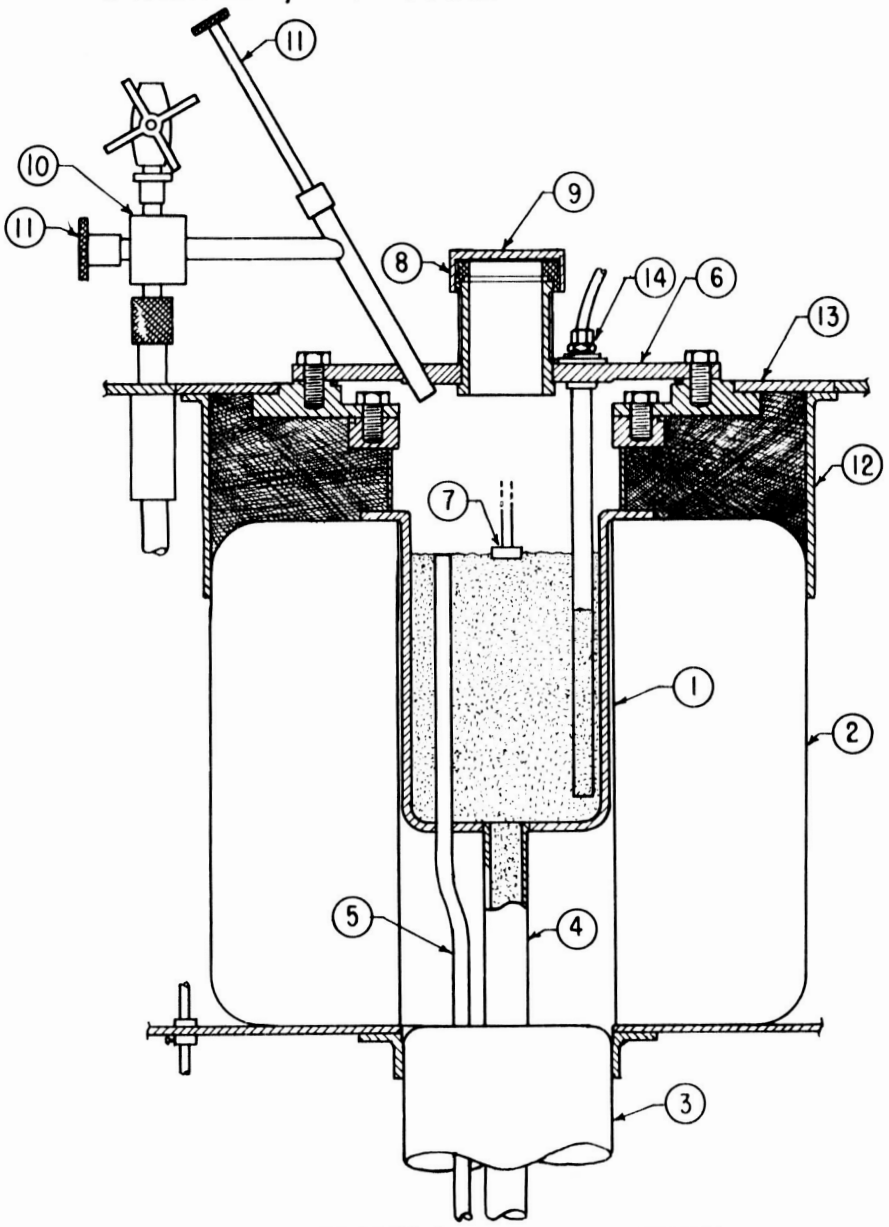

FIGURE 8. RETORT ASSEMBLY FOR NEW FACILITY

FIGURE 8. RETORT ASSEMBLY FOR NEW FACILITY

1. SODIUM RETORT
2. RETORT FURNACE
3. CLAMP SHELL FURNACE
4. SODIUM DRAIN AND FILL TUBE
5. SODIUM DRAIN TUBE
6. RETORT HEAD
7. TEST SPECIMAN (LEVEL INDICATOR)
8. EXTENSION TUBE
9. CAP
10. COVER GAS AND VACUUM PIPING
11. SODIUM "ROD-OUT" TUBES
12. INSULATION
13. DRY BOX BOTTOM
14. THERMOCOUPLES

HYDRONAUTICS, INCORPORATED

These drums can take pressures of 1 to 30 psia and be heated to 300°F without damage or danger. In the sodium system under discussion two such drums are provided; one is used for storage and the other is used for a drain tank. When the spent sodium fills the drain tank, it is shipped back to the supplier for reprocessing or discarding. In order to further purify the liquid sodium to 10 ± 10 ppm oxide content, it is hot trapped in a special charging tank containing zirconium chips. In this tank a small charge of 25 pounds of sodium is transferred from the storage tank. This charge is then heated to 1400°F for a period of 72 hours in a special furnace described later. The zirconium turnings act as an oxygen gettering material which gradually reduces the oxides in the liquid metal and converts them to the stable zirconium oxide. After gettering, the charging tank is used as a small storage tank to fill the retort periodically. After each test run, the sodium in the retort is drained to the drain tank by means of gas pressure and vacuum control. A schematic diagram of the sodium system is shown in Figure 9. All standard safety precautions have been observed such as providing metal pans under all sodium containing apparatus, safety goggles, breathing masks and appropriate fire extinguishers.

3. Magnetostriction Apparatus - The components associated with this system are the magnetostriction transducer and related electronic powering and measuring equipment (described previously), tubular housing, elevating mechanism and retort sealing system with its instrumentation and controls.

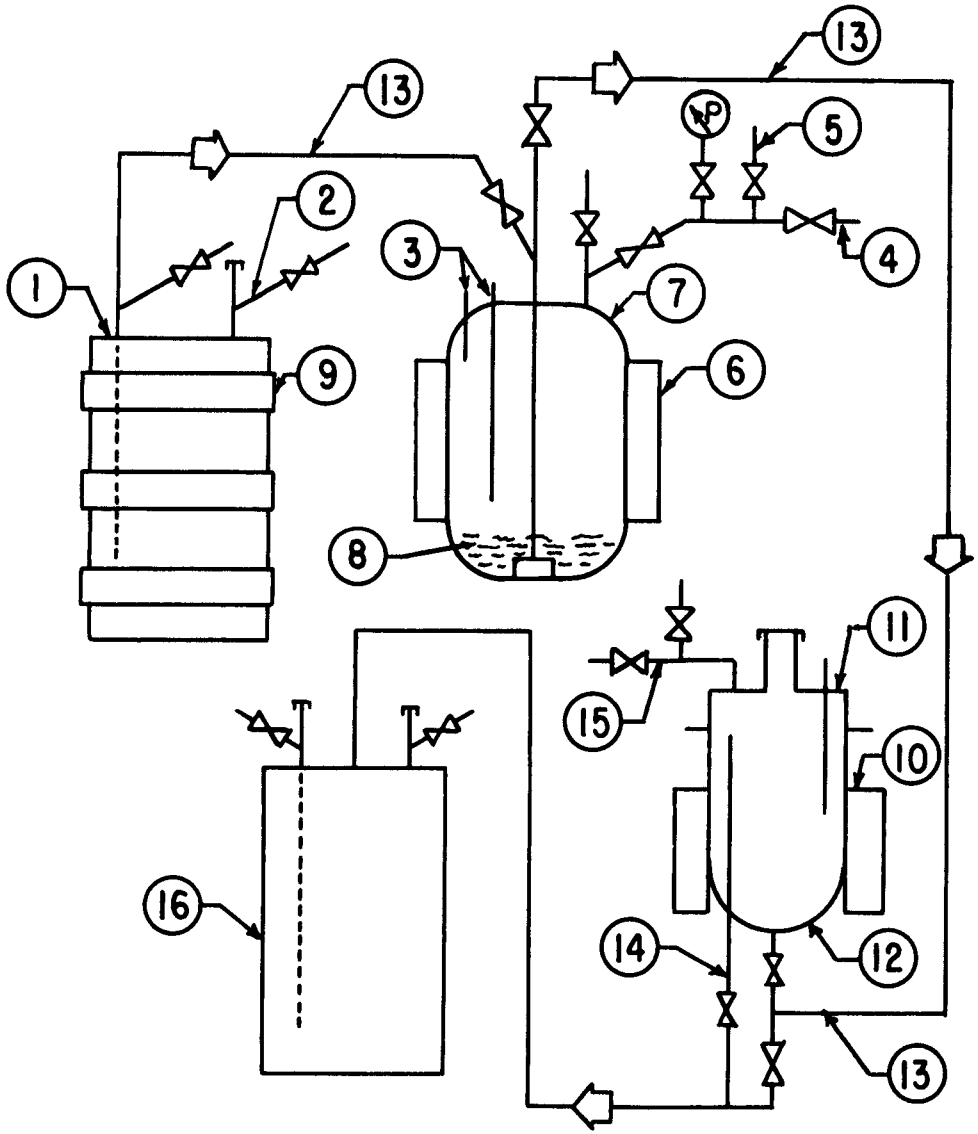

1. SODIUM DRUM (30 GALLON)
2. COVER GAS INLET
3. THERMOCOUPLE WELLS
4. VACUUM INLET
5. COVER GAS INLET
6. HEATER
7. CHARGE TANK & HOT TRAP (25 POUND)
8. GETTERING MATERIAL (ZIRCONIUM OXIDE)
9. BAND HEATERS
10. RETORT FURNACE
11. RETORT COVER
12. RETORT
13. SODIUM FILL LINE
14. SODIUM DRAIN LINE
15. COVER GAS, VACUUM, & GAGE LINE
16. SODIUM DUMP DRUM (30 GALLON)

FIGURE 9. SCHEMATIC SODIUM METALS LOOP FOR NEW FACILITY

(a) Tubular Housing and Elevating Mechanism - The transducer and horn assembly is mounted into a vacuum tight tubular housing by means of machining the nodal support flange on the upper horn cylinder to accomodate an O-ring seal within the housing. The support flange is so arranged that it electrically isolates the horn from the housing. The tubular housing pierces the dry box through an O-ring seal gland which is readily removable for renewal of worn seal rings. The tubular housing is fitted into a well recess which is welded integrally with the dry box. The top of the tubular housing forms a crosshead which travels up and down on a pair of external ball bearing jack screws which are powered by a gear motor drive. The internal volume of the tubular housing is filled with kerosene which submerges the transducer stack. An additional seamless tubular water cooling coil is positioned around the transducer to dissipate the heat generated by the power to the magnetic coils. The entire elevating mechanism is operated by a foot switch outside the dry box. Limit switches are provided to prevent over-travel of the crosshead. A mechanical indicator on the housing shows depth of specimen immersion in the liquid sodium, after surface contact (electrical indication) is made.

The lower portion of the housing contains the male telescopic seal which mates with the retort telescopic seal to make a vapor tight joint during an experiment. The assembly details of this component are shown in Figure 10.

When magnetostriction tests are not in progress, or when the instrument is being calibrated, a vacuum tight screw cap is provided to seal the retort telescopic opening. Calibration of

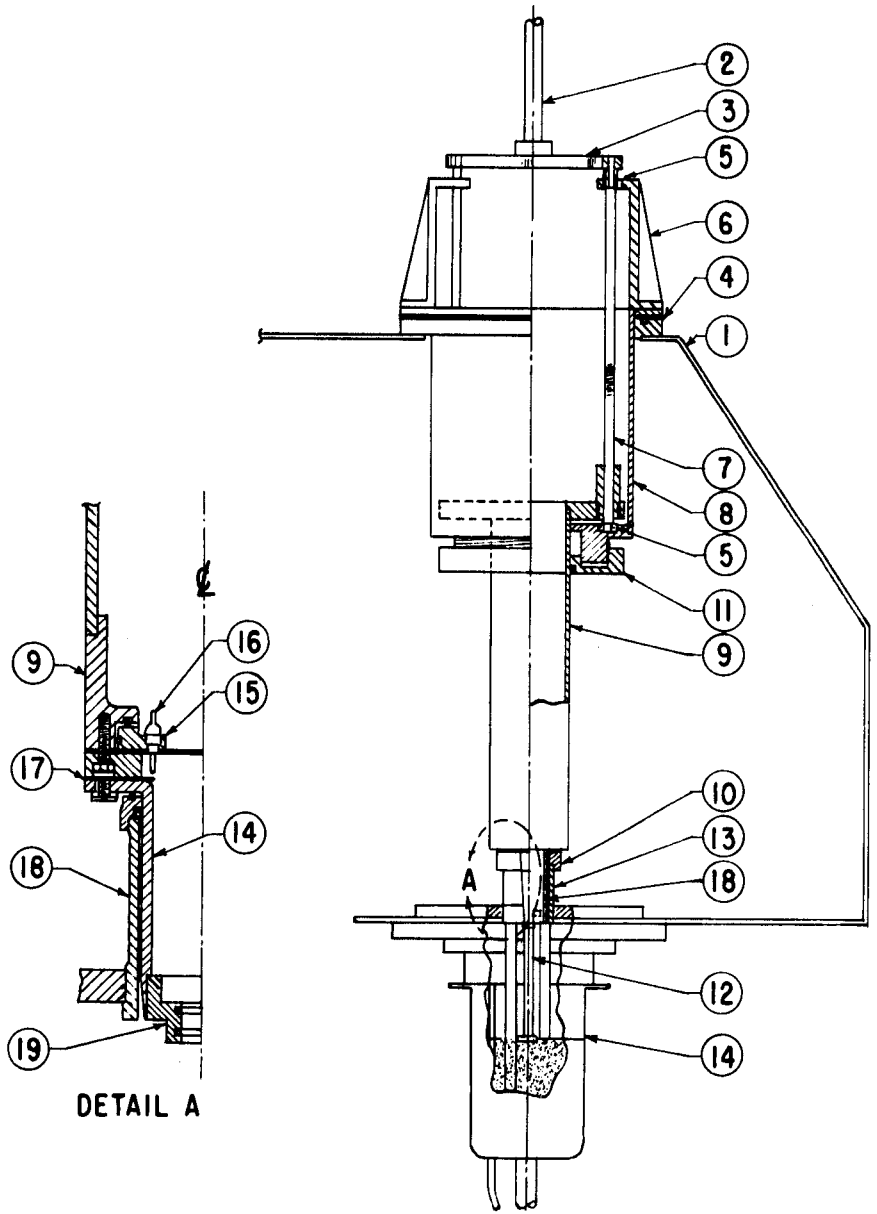

FIGURE 10. ELEVATING MECHANISM AND TUBULAR HOUSING FOR NEW FACILITY

1. REFRACTORY METALS DRY BOX
2. DRIVE SHAFT
3. SPUR GEARS
4. SEAL-ELEVATING HOUSING
5. RADIAL BEARING
6. BEARING SUPPORT
7. BALL BEARING JACK SCREW
8. ELEVATING MECHANISM HOUSING
9. TRANSDUCER HOUSING
10. SEAL-TRANSDUCER HOUSING
11. COMPRESSION CAP
12. MAGNETOSTRICTION HORN
13. MALE TELESCOPIC SEAL (HOUSING)
14. RETORT ASSEMBLY
15. NODAL FLANGE (INSULATED)
16. CERAMIC THRU-SEAL
17. MICARTA INSULATION
18. FEMALE TELESCOPIC SEAL (RETORT)
19. VOICE PICK-UP COIL SUPPORT

FIGURE 10. ELEVATING MECHANISM AND TUBULAR HOUSING FOR NEW FACILITY

the magnetostriction device is accomplished in place through the large access door in the rear.

4. Heating System - The components associated with the heating system are the retort furnace, hot-trap furnace, vacuum furnace, drum heaters, and traced lines with related instrumentation and controls. An electrical schematic diagram of this system is shown in Figure 11.

(a) Retort Furnace - The retort furnace is a modified pot furnace (2500 watts), with the base removed,as used in the initial test facility. The original furnace was designed for pot temperatures of 1500°F. However,with the addition of the retort piping, a booster clamp-shell furnace is fitted around the bottom of the piping leaving the retort. The retort and clamp-shell furnaces are supported on an adjustable shelf mounted underneath the dry box.

(b) Hot-trap furnace - This furnace is a 16 kw 10 inch diameter pot furnace, dolly mounted and adapted to receive the hot trap charging tank. The retort and hot trap furnaces are regulated by an automatic pyrometer which can maintain the retort temperatures within ± 15°F.

(c) Vacuum Furnace - The dry box was adapted to receive a 15 inch I.D. "air lock" which can be converted to a large vacuum furnace should the need be required. The dry box was also fitted with a smaller 6 inch I.D. specimen air lock to allow for rapid movement of specimens in and out of the dry box. For the initial work, the specimen lock is fitted with external heater

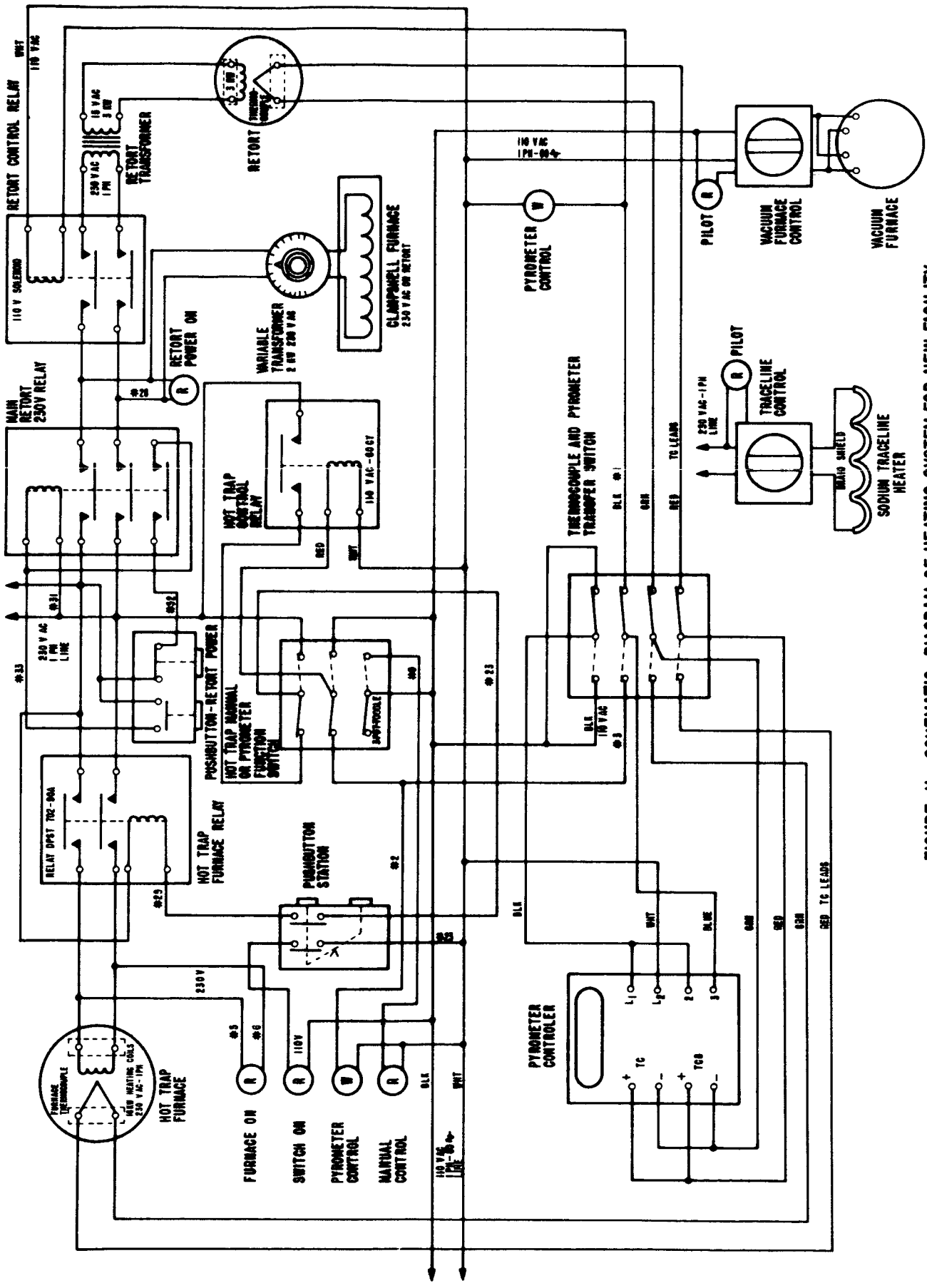

FIGURE II -SCHEMATIC DIAGRAM OF HEATING SYSTEM FOR NEW FACILITY

elements to provide vacuum bake out of refractory metals prior to testing, since minor traces of moisture can seriously interfere with the results.

(d) Drum Heaters - Two band heaters of 2000 watts are used around the storage drum to liquefy the sodium, for transfer to other parts of the system. A single band heater is used to keep the drain drum warm during use.

(e) Traced Lines - The sodium transfer lines are traced with spirally wrapped wire heating elements clipped in place with hose clamps. Thermocouples are provided at convenient points to indicate temperatures.

5. Cooling System - The components associated with the cooling system are the pump and heat exchange systems with related instrumentation and controls. These are shown in Figure 12.

6. Safety Controls - All major controls are brought out to front panels by means of reach rods for easy access and operation. Main control valves and circuits such as vacuum, sodium, cover gas, cooling and heating, operate pilot lights to indicate "in use". Safety interlocks are provided to prevent cover gas system and vacuum, cooling water and vacuum, or sodium and vacuum systems from operating simultaneously. Alarms will be provided to indicate loss of cover gas pressure, coolant pressure, excess O_2 or moisture content in cover gas, loss of contact of specimen with sodium and overheating of furnaces. Figures 13, 14, 15 and 16 are photographs of the new facility as installed.

1. COOLING WATER PUMP
2. PRESSURE REDUCING VALVE
3. PRESSURE-IN GAUGE
4. TEMPERATURE-IN GAUGE
5. COOLING BAFFLES
6. DRY BOX FALSE BOTTOM
7. TEMPERATURE-OUT GAUGE
8. COOLING WATER TANK
9. ELEVATING MECHANISM
10. COOLING WATER COILS
11. TEMPERATURE-OUT GAUGE

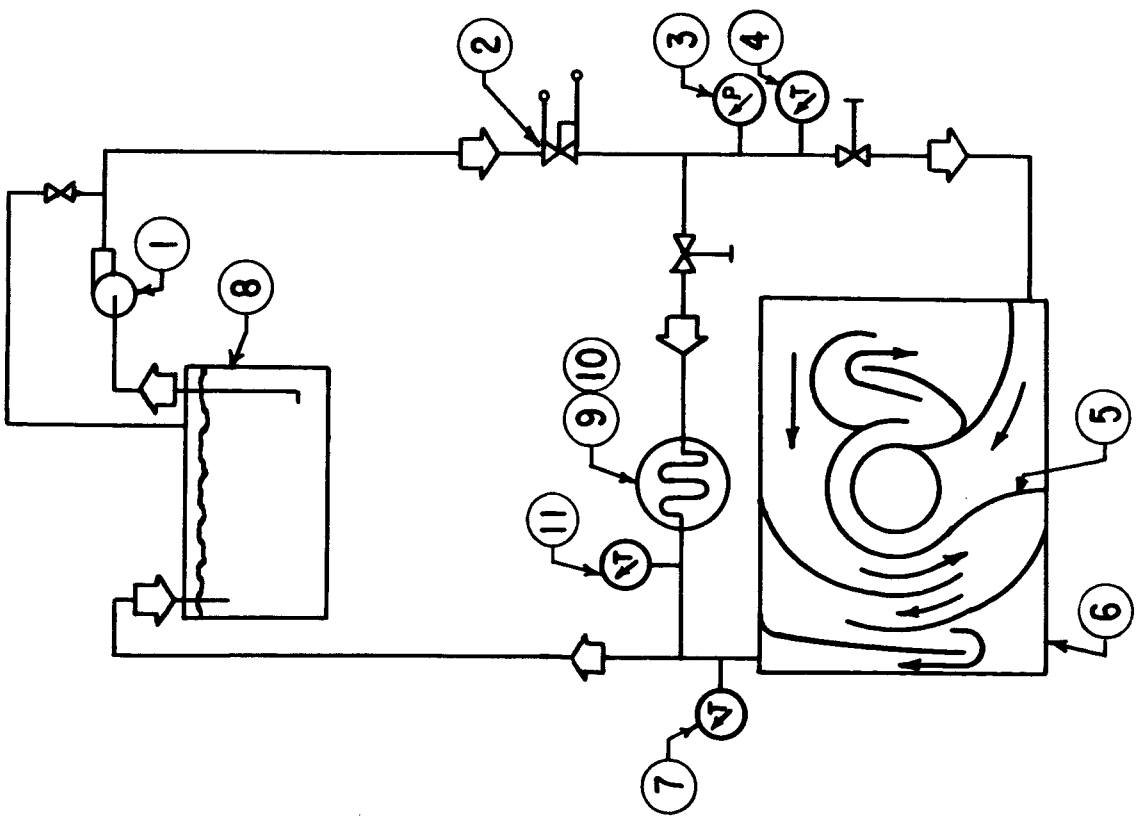

FIGURE 12. SCHEMATIC COOLING SYSTEM FOR NEW FACILITY

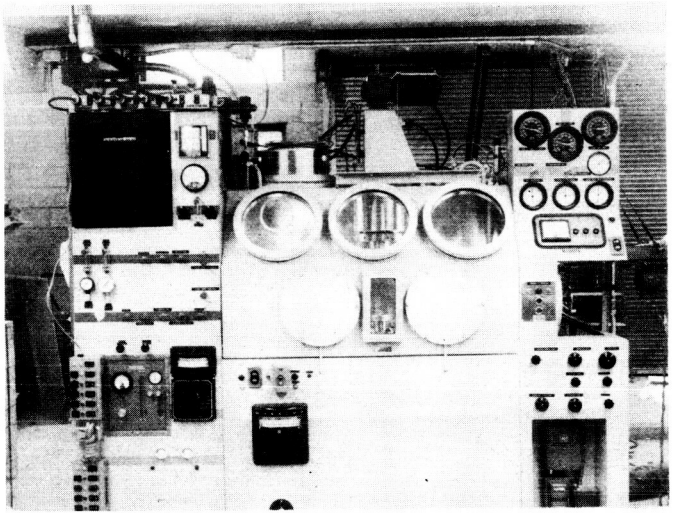

FIGURE 13. FRONT VIEW OF REFRACTORY METALS DRY BOX FACILITY SHOWING INSTRUMENTATION AND GENERAL ARRANGEMENT

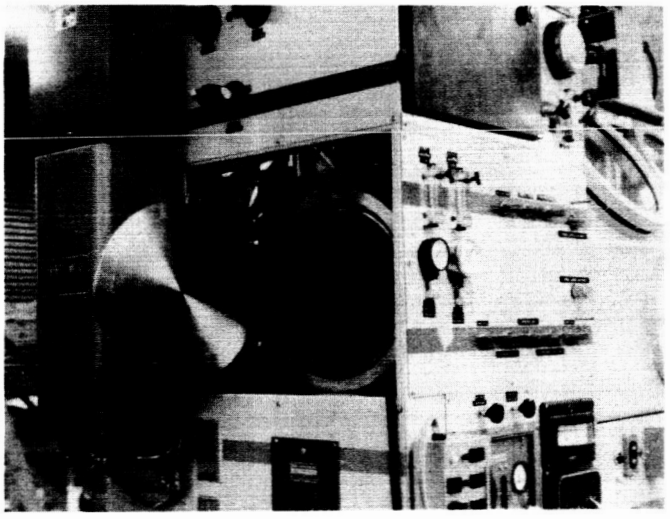

FIGURE 14. RIGHT SIDE VIEW OF REFRACTORY METALS DRY BOX FACILITY SHOWING AIRLOCK AND COVER GAS SYSTEM

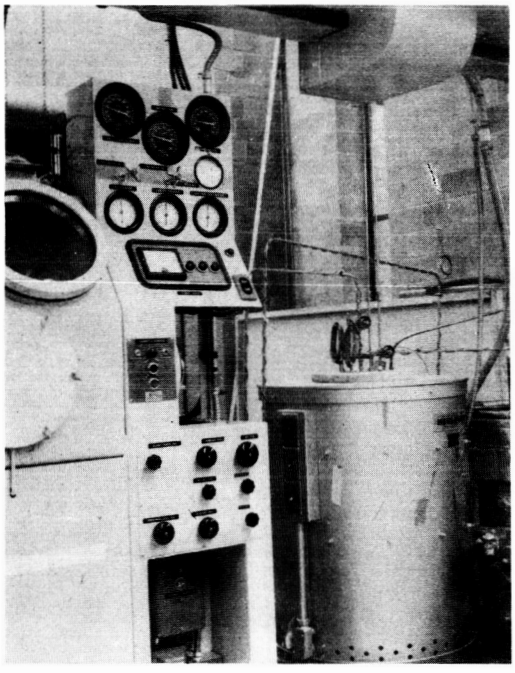

FIGURE 15. LEFT SIDE VIEW OF REFRACTORY METALS DRY BOX SHOWING VACUUM AND SODIUM SYSTEMS

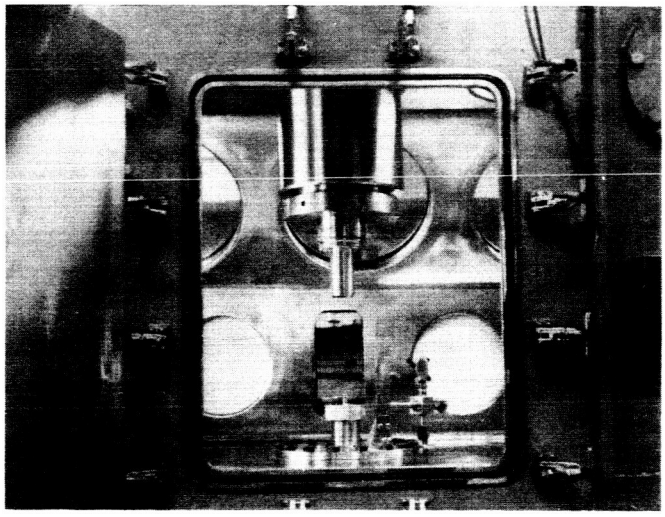

FIGURE 16. REAR VIEW OF REFRACTORY METALS DRY BOX WITH ACCESS DOOR OPEN SHOWING MAGNETOSTRICTION DEVICE AND RETORT ASSEMBLY

RESULTS AND DISCUSSION

Effect of Testing Time on the Rate of Cavitation Damage

It has been the general practice in the past to test all materials over an arbitrarily selected constant duration, and to compare the cumulative weight loss as an indication of the cavitation damage resistance. Recent investigations with the help of a magnetostriction oscillator, using distilled water at 80°F as the test liquid, have pointed out that this is not a good practice since the rate of damage is dependent on the test duration itself (8), (9). This result has been confirmed for the case of liquid sodium using five metals (pure iron, 201 nickel, 316 stainless steel, 600 inconel, 100A titanium). The data are shown in Figures 17 through 21*. An analysis of these figures shows that the relationship between the rate of cavitation damage and the test duration can be divided into four zones as follows:

(a) Incubation Zone. In this zone there is no measurable weight loss. The extent of this zone depends upon the amplitude of vibration for a given frequency and temperature.

(b) Accumulation Zone. This zone represents the time during which the rate of weight loss increases with time as a result of an apparently increasing energy absorption rate.

(c) Attenuation Zone. The rate of weight loss reaches a peak value and then decreases with time due to the attenuation of the energy absorption rate. The beginning of this zone is

* The amplitudes referred to in this report are all peak to peak values.

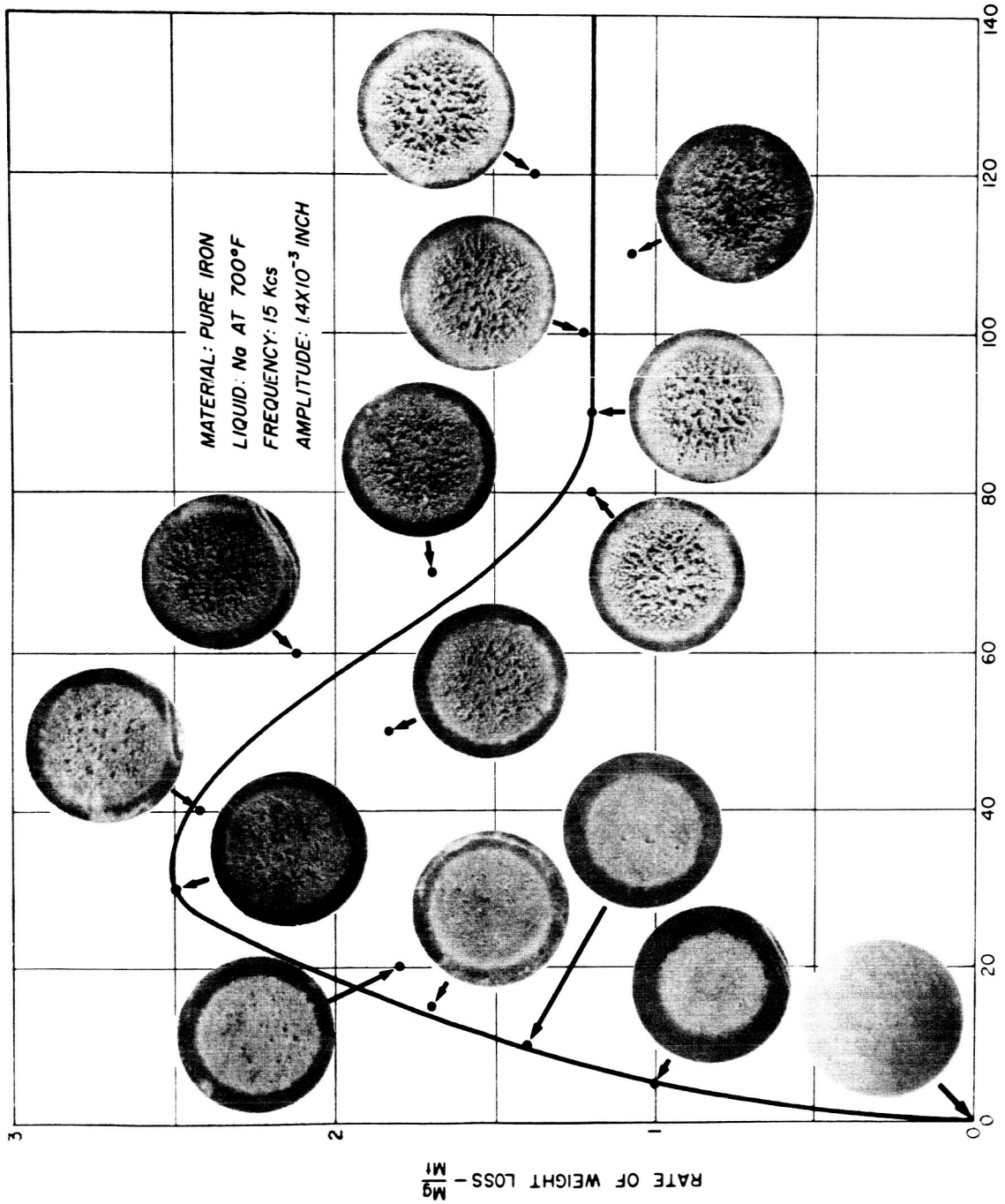

FIGURE 17. EFFECT OF TIME ON RATE OF WEIGHT LOSS OF PURE IRON

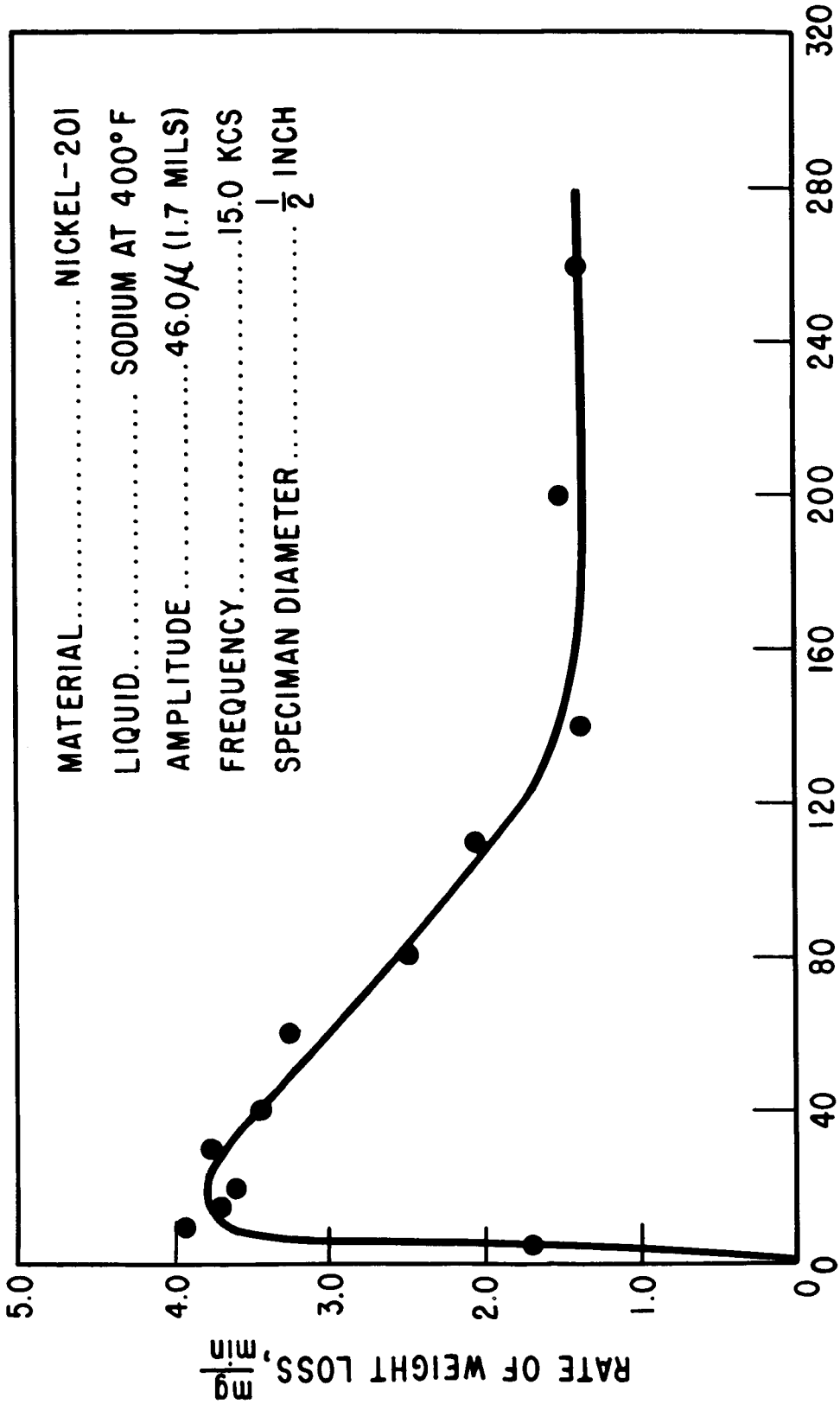

FIGURE 18. EFFECT OF TIME ON RATE OF WEIGHT LOSS OF 201 NICKEL

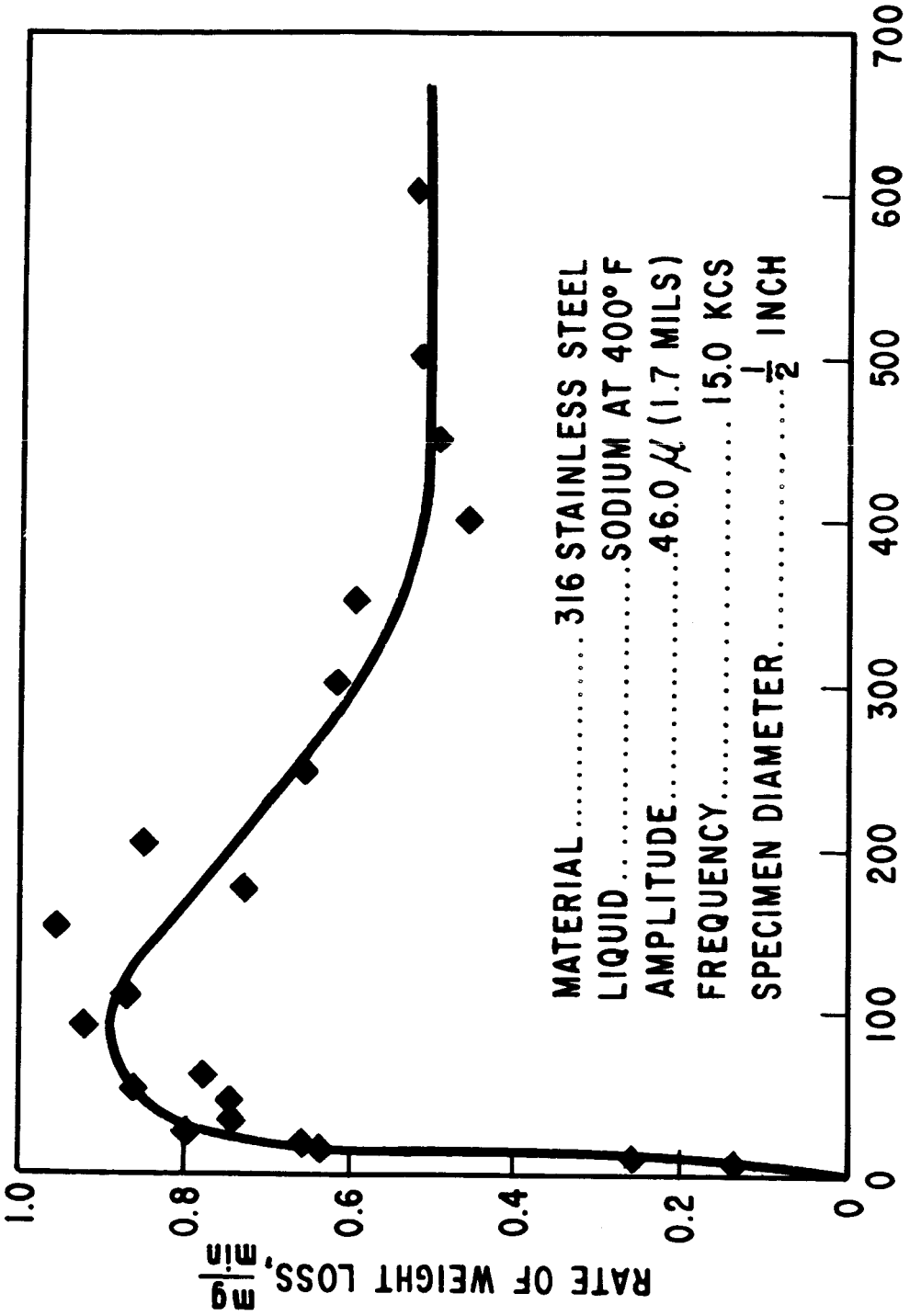

FIGURE 19. EFFECT OF TIME ON RATE OF WEIGHT LOSS OF 316 STAINLESS STEEL

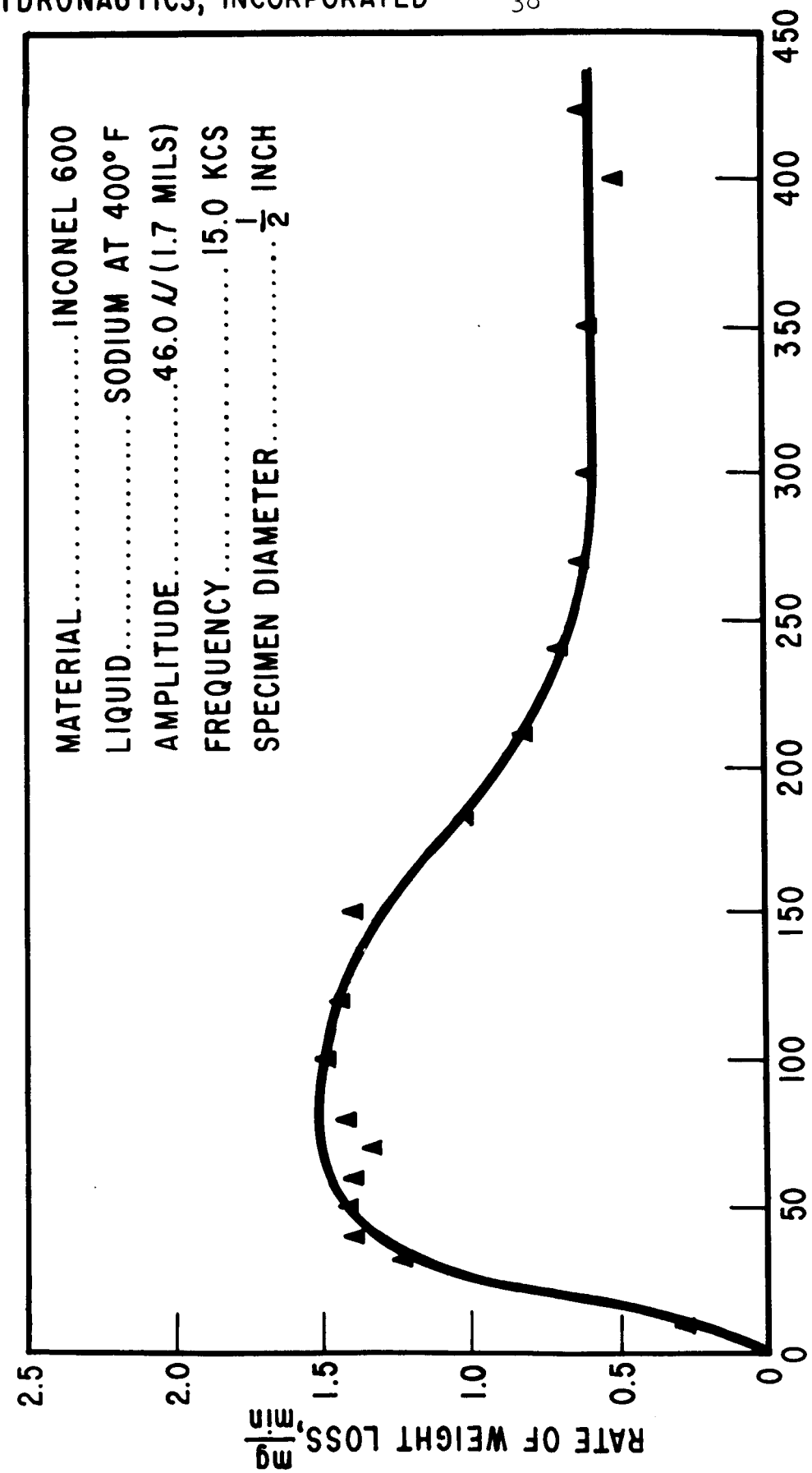

FIGURE 20. EFFECT OF TIME ON RATE OF WEIGHT LOSS OF 600 INCONEL

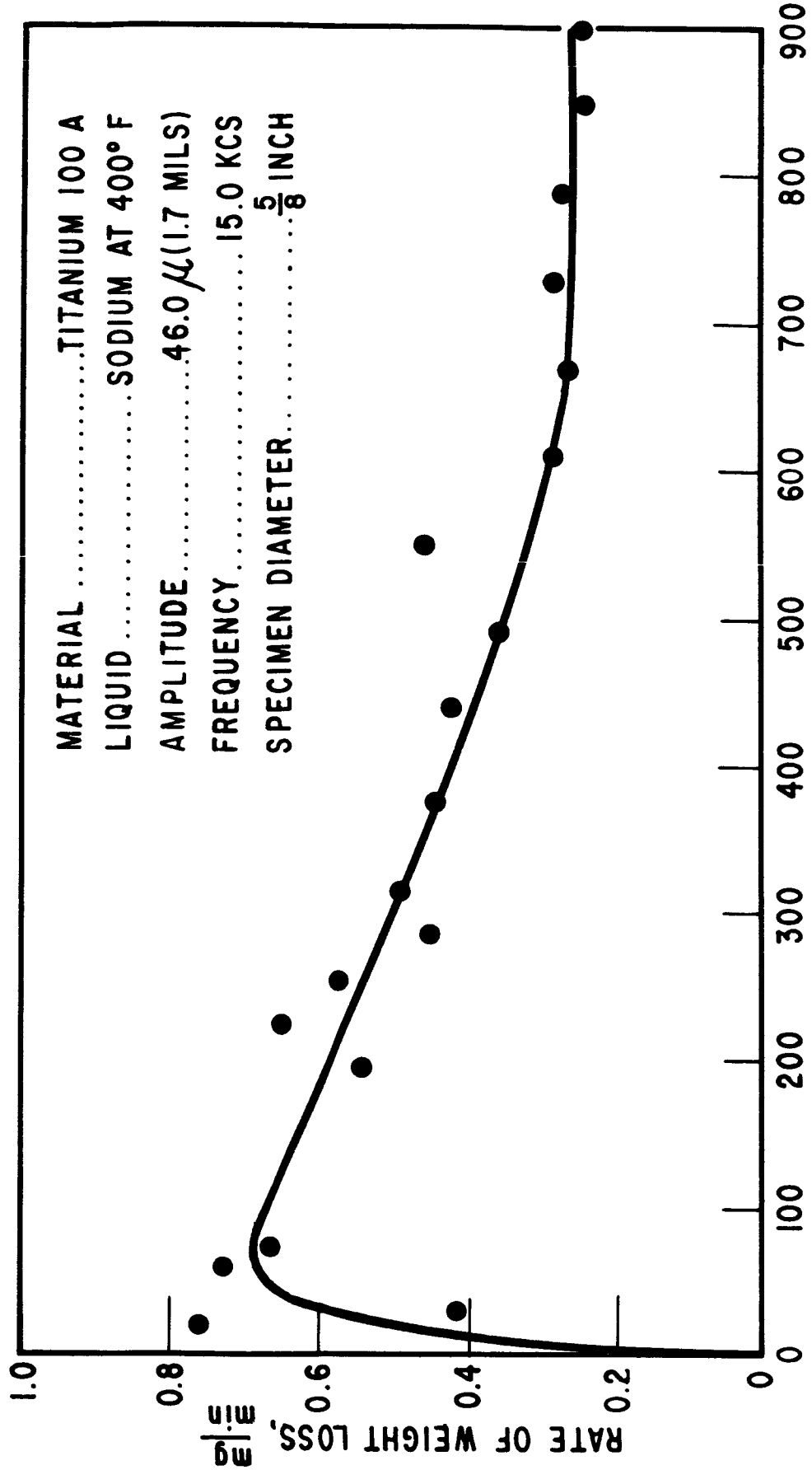

FIGURE 21. EFFECT OF TIME ON RATE OF WEIGHT LOSS OF 100 A TITANIUM

characterized by the formation of isolated deep craters on the surface of the test material.

(d) Steady State Zone. Since the rate of loss reaches a constant value after the attentuation zone, this is called the steady state zone.

The interacting influence of testing time has to be properly understood before any attempt is made to compare the cavitation damage resistance of different materials under different test conditions. It seems logical to test all materials until they reach the steady state zone.

Effect of Displacement Amplitude on the Rate of Cavitation Damage

Recent investigations with distilled water at 80°F showed that the cavitation damage rate varied as the square of the displacement amplitude (8). It has been confirmed that this relationship is also true for the case of liquid sodium at 400°F. The cavitation damage rates in the steady state zone for five metals (pure iron, 201 nickel, 316 stainless steel, 600 inconel and 100A titanium) are shown as a function of amplitude in Figure 22. This relationship is:

$$\frac{r}{\rho} = c_1 a^2 \qquad [1]$$

where

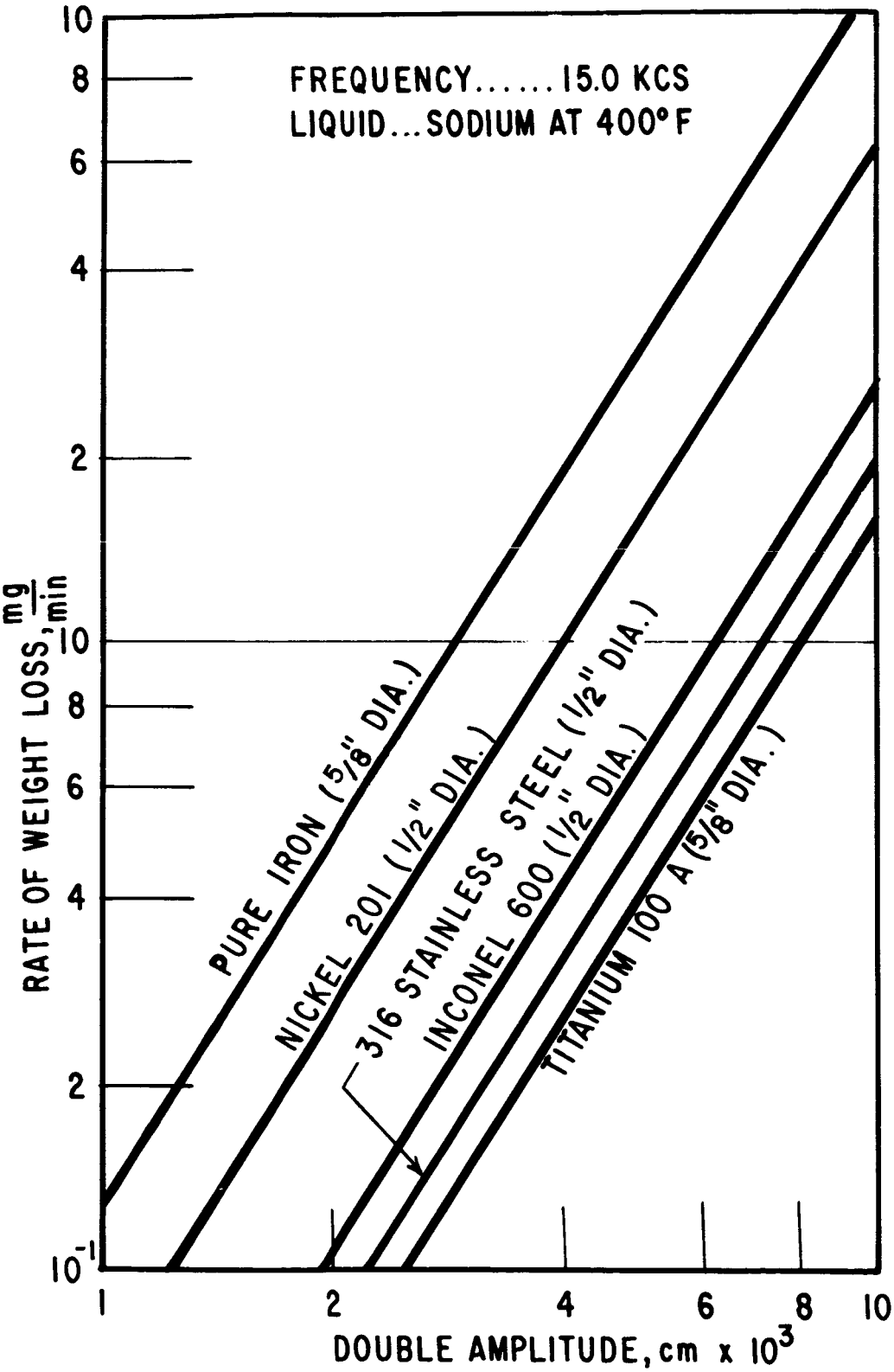

FIGURE 22. EFFECT OF DISPLACEMENT AMPLITUDE ON THE RATE OF WEIGHT LOSS

r is the rate of weight loss

a is the amplitude of vibration

ρ is the density of material

c_1 is an experimental constant

Average values of the constant c_1 for each material tested are presented in Table 1 along with their typical mechanical properties as obtained from the literature. It is not obvious as to why the damage rate should vary as the square of the amplitude. However, an analysis of the bubble collapse energies in terms of the amplitude of oscillation should explain this relationship.

Effect of Liquid Metal Temperature on the Rate of Cavitation Damage

One of the basic parameters in the study of cavitation damage in liquid metals is the temperature of the liquid metal. Quantitative results have been obtained on the effect of temperature up to 1000°F in the steady state zone as shown in Figure 23 for 100A titanium. This result confirms that obtained by Peters and Rightmire (10), Leith (11), and Plesset (12) using water as the test liquid. The behavior of a given material in a cavitating liquid environment as a function of temperature is difficult to explain on the basis of this limited information. It is obvious that the liquid metal properties, as well as the test material properties, are affected by a change in the liquid metal temperature and a detailed investigation is necessary to understand this effect.

TABLE 1

Mechanical Properties and Cavitation Damage
Resistance of Materials Tested

	Y.S. psi x 10^{-3}	T.S. psi x 10^{-3}	Elongation %	BHN *	Strain Energy g/cm^2 x 10^{-3}	Damage Rate mgs/min
316 S.S.(1)	29.0	74.75	51	135-185(2)	1770	0.55
Nickel 201(3)	12.0	44.0	51	90-120(4)	1002	1.32
Inconel 600(5)	31.0x	90.5x	46x	123-175	1940	0.58
Pure Iron(7)	55.6	65.6	26.5	82-100	1134	1.5
Ti 100-A(8)	———	———	———	———	———	0.345

* - Indicates Data taken at room temperature

x - Indicates Data taken at 600°F, all other data at 400°F

TABLE 1 (Concluded)

	Density gm/cm^3	Amplitude $cm \times 10^3$	C_1 cm/min	Intensity $watts/cm^2 \times 10^4$	Reciprocal of Rate of Volume Loss $\frac{1}{cm^3/sec} \times 10^{-6}$
316 S.S.(1)	8.9	4.6	2.9	1.78	0.97
Nickel 201(3)	8.9	4.6	7.0	2.57	0.38
Inconel 600(5)	8.43	4.6	3.25	2.29	0.90
Pure Iron(7)	7.86	4.6	9.0	2.28	0.49
Ti 100-A(8)	4.54	4.6	3.6	——	——

(1) "Steels for Elevated Temperature Service," United States Steel, Fourth Printing, 1961, p. 46.

(2) "Alloy Digest," Engineering Alloys Digest, Inc., Filing Code SS-114, February 1961.

(3) Thompson, J. G., "Nickel and its Alloys" National Bureau of Standards Circular 592, U. S. Dept. of Commerce, February 1958, p. 25.

(4) "Engineering Properties of Nickel," Technical Bulletin T-15, Huntington Alloy Products Division, The International Nickel Company, Inc., February 1960.

(5) "Engineering Properties of Inconel Alloy 600", Technical Bulletin T-7, Huntington Alloy Products Division, The International Nickel Company, Inc.,1961, p. 46.

(7) Taylor, L., Editor, Metals Handbook, American Society for Metals, 1948 Edition, p. 432.

(8) Mantell, C. L., Editor, Engineering Materials Handbook, First Edition, McGraw-Hill Book Company, 1958, p. 13-49.

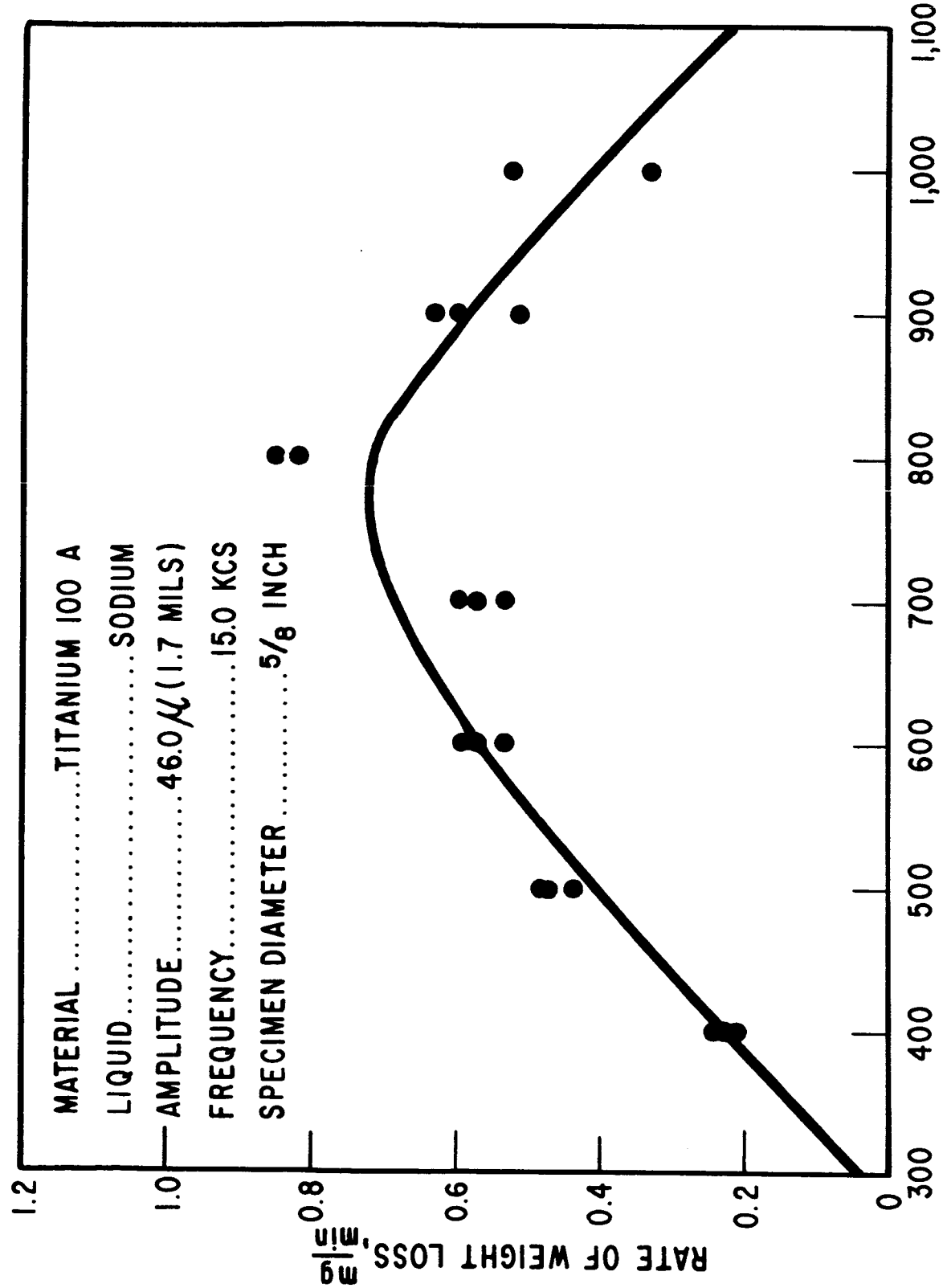

FIGURE 23. EFFECT OF LIQUID METAL TEMPERATURE ON RATE OF WEIGHT LOSS

Effect of Mechanical Properties on the Rate of Cavitation Damage

There have been many attempts in the past to correlate the mechanical properties of the test material with cavitation damage (10, 13, 14, 15). Recent efforts to correlate the strain energy of the material (area of the engineering stress-strain diagram from a simple tensile test) have offered the best promise (14, 15). From the beginning, these efforts have been handicapped by the lack of actual stress-strain information even for tests at room temperature. In fact, complete engineering stress-strain curves are a rarity (16) at room temperatures. At higher temperatures, these attempts to obtain actual strain energies become much more difficult. However, the typical values of ultimate tensile strength, yield strength and ultimate elongation can be obtained from published literature (17, 18, 19, 20) as a function of temperature for four of the five metals tested. It was decided to use these reported values to estimate the magnitude of strain energy by the use of the following approximate relationship:

$$S_e = \frac{(Y + T)}{2} \epsilon \qquad [2]$$

where

Y is the yield strength

T is the ultimate tensile strength

ϵ is the ultimate elongation.

Such estimated values of the strain energy are shown as a function of temperature in Figure 24. The relationship between the reciprocal of the rate of volume loss due to cavitation damage in liquid sodium at 400°F and the estimated strain energy of the material at 400°F is shown in Figure 25. Considering the fact that these values of mechanical properties are only typical values and that they may vary from heat to heat, the correlation between the estimated strain energy and the cavitation damage resistance is good. This result points out the need for conducting the actual stress-strain and other mechanical property tests at the temperature of interest on the particular samples of metal from which the cavitation damage specimens are made.

Order of Magnitude of Intensity of Cavitation Damage in Liquid Sodium at 400°F

A reasonably successful formulation of the concept of absolute intensity of cavitation damage has been accomplished recently (9). It is generally accepted that a portion of the bubble collapse energy is absorbed by the test material, causing final fracture and volume loss. The energy absorbed by the material E_a is given by:

$$E_a = \Delta V \cdot S_e' \qquad [3]$$

where ΔV is the volume loss and S_e' is the strain energy defined as the energy absorbed per unit volume of the material up to complete fracture under this type of loading. Hence, the power

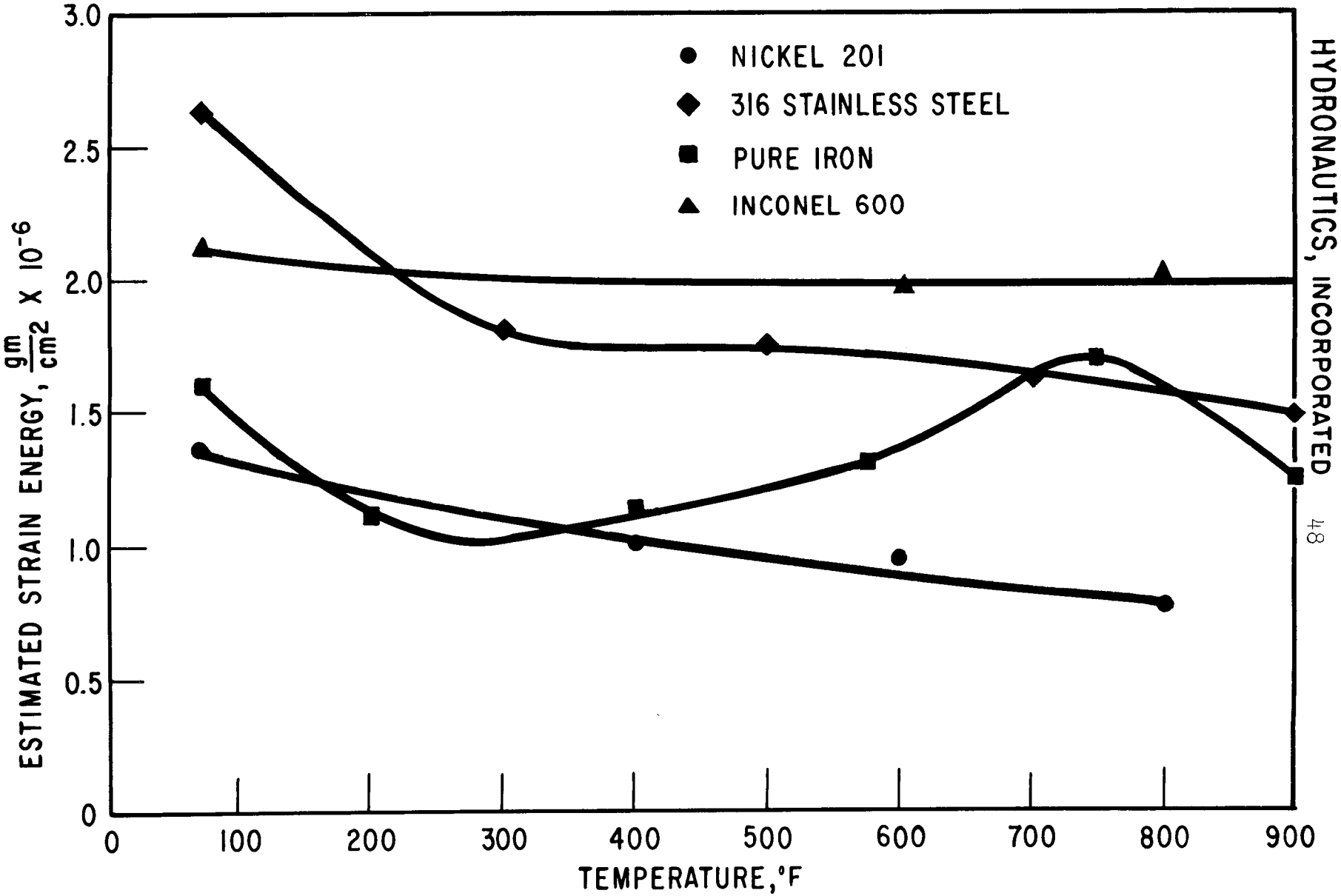

FIGURE 24. EFFECT OF TEMPERATURE ON ESTIMATED STRAIN ENERGY

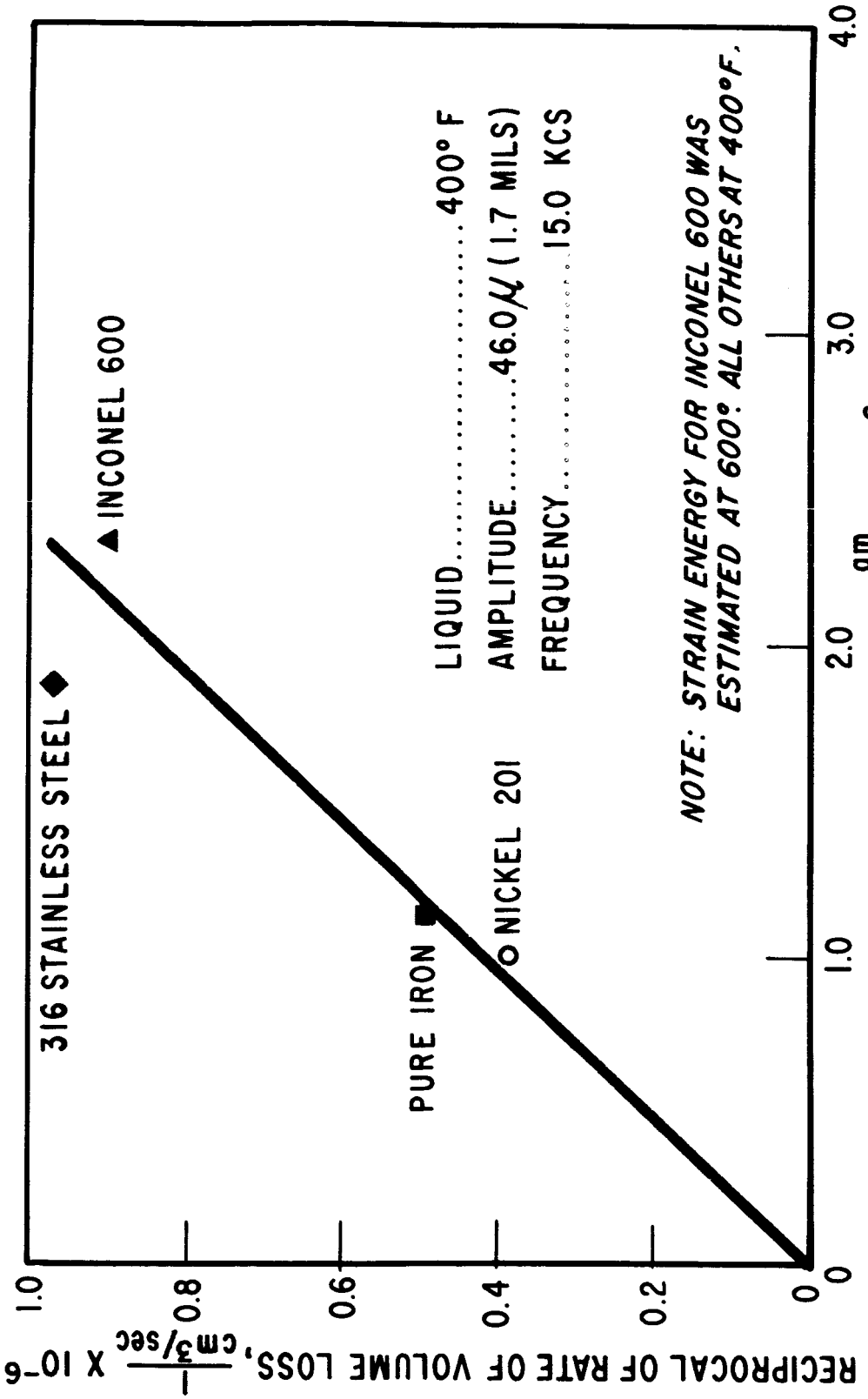

FIGURE 25. RELATIONSHIP BETWEEN THE ESTIMATED STRAIN ENERGY AND THE RECIPROCAL OF THE RATE OF VOLUME LOSS

any given temperature. There are two limitations to this approach. The average rate of depth of erosion is time dependent. Secondly, the value of S_e' is not precisely known at present. In the present investigations, an approximate analysis was made to determine I in watts per square centimeter for liquid sodium at $400^{\circ}F$ in the steady state zone using the strain energy values as obtained by Equation [2] and as shown in Figure 24. The computed value of I for each material is shown in Table 1. The average value of cavitation damage intensity in liquid sodium at $400^{\circ}F$ is approximately 2.3×10^{-4} watts/cm^2 as compared to an estimated value of 1.5×10^{-4} watts/cm^2 in distilled water at $80^{\circ}F$ for a double amplitude of 1.5×10^{-3} inch and a frequency of 15 kcs. The intensity of damage in liquid sodium at $400^{\circ}F$ is about one and one half times that in distilled water at $80^{\circ}F$.

High Frequency Fatigue Testing

The above analysis points out the need for obtaining actual mechanical property data at the frequency and temperature of tests in liquid sodium. One of the relatively easy methods of obtaining these data is by the high frequency fatigue tests making use of the magnetostriction apparatus used for cavitation damage tests.

This method has been the subject of investigation recently by Mason (5), Neppiras (21) and Tanaka (22), and it appears ideally suited since the strain rates are of the order of those encountered in the cavitation damage process under study. In addition, the rapidity of the test permits extensive studies to

absorbed by the material is given by:

$$P_a = \frac{\Delta V \cdot S_e'}{t} \qquad [4]$$

where $\Delta V/t$ is the volume loss per unit time. In order to take into consideration the effect of size of the system the power absorbed per unit area is defined as the intensity of cavitation damage.

Hence,

$$I = \frac{P_a}{A_e} = \frac{\Delta V \cdot S_e'}{A_e \cdot t} \qquad [5]$$

$$\boxed{I = \frac{i\, S_e'}{t}} \qquad [6]$$

where I is the intensity of cavitation damage, A_e is the area of erosion and i is the average depth of erosion.

With the help of this definition, it now seems possible to make a quantitative comparison of the intensities of damage in high temperature liquid metals with those of room temperature water test systems and with those of practical hydrodynamic systems. The value of I can be easily computed based on the average depth of erosion per unit time and the energy absorbed by the unit volume of the material up to fracture by this type of loading at

be made. At 15 kcs, the limiting number of cycles, set at 10^8, can be achieved in two hours.

The specimen selected for the fatigue studies is shown in Figure 26. The basis of design of this type of fatigue specimen is as follows (22). The solution of the one dimensional wave equation for a wave travelling in a stepped cylindrical rod with diameter d_1, over a length ℓ, and diameter d_2 over a length ℓ_2 is given by

$$\tan k\ell_1 + p \tan k\ell_2 = 0$$

where

$$k = \frac{2\pi f}{c}, \quad p = \frac{d_1^2}{d_2^2} \qquad [7]$$

f = frequency

c = velocity of sound in the material.

The solution of Equation [7] is obtained graphically as shown in Figure 27. Since an abrupt change in the diameters would produce stress concentrations, a smooth tapered transition is provided. The altered length ℓ_2 due to this transition is experimentally determined by adjusting the length.

The specimen was calibrated by measuring the displacement amplitude along the specimen by means of a microscope and by plotting the amplitude as a function of the longitudinal

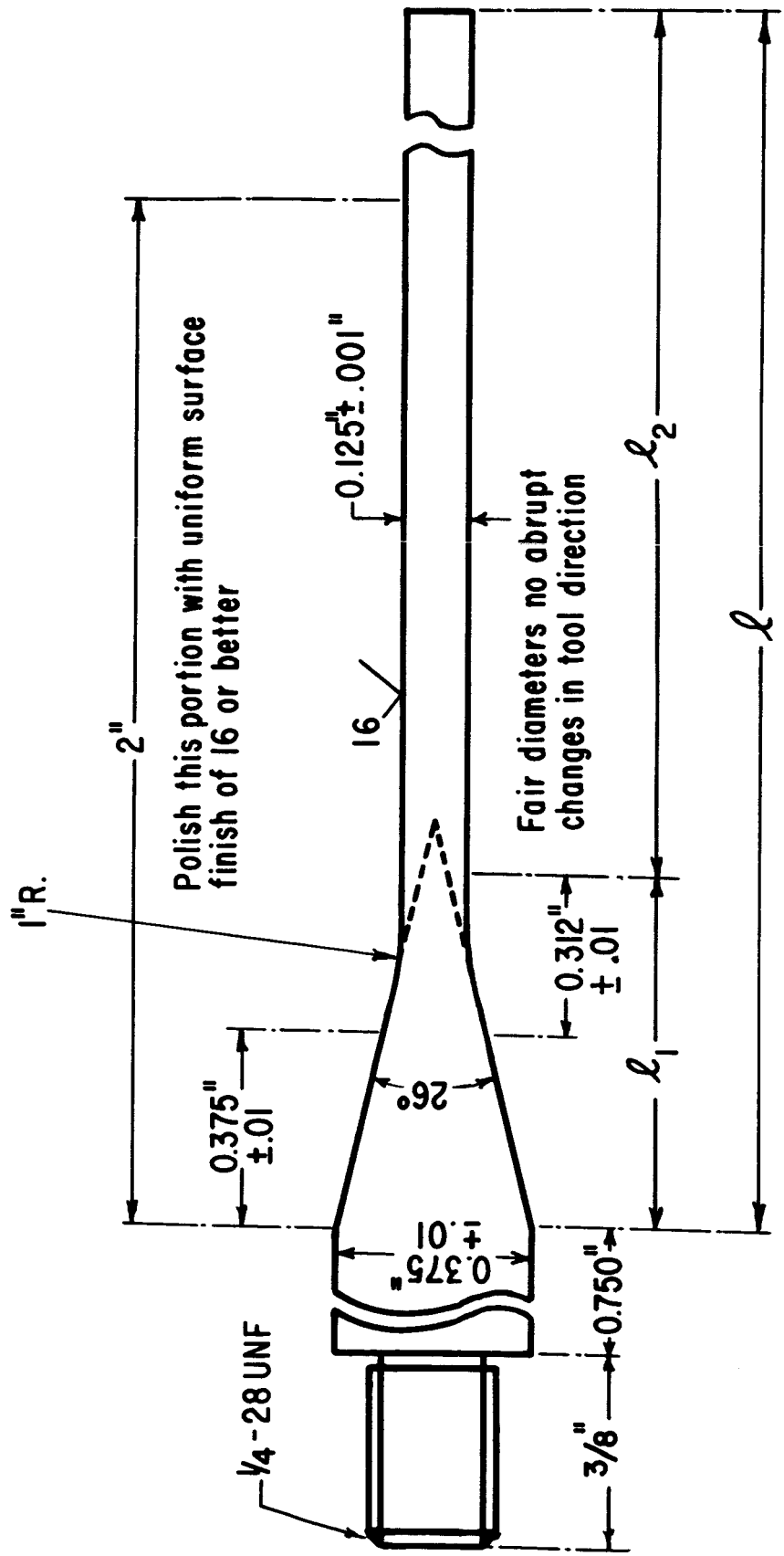

FIGURE 26. HIGH FREQUENCY FATIGUE SPECIMAN

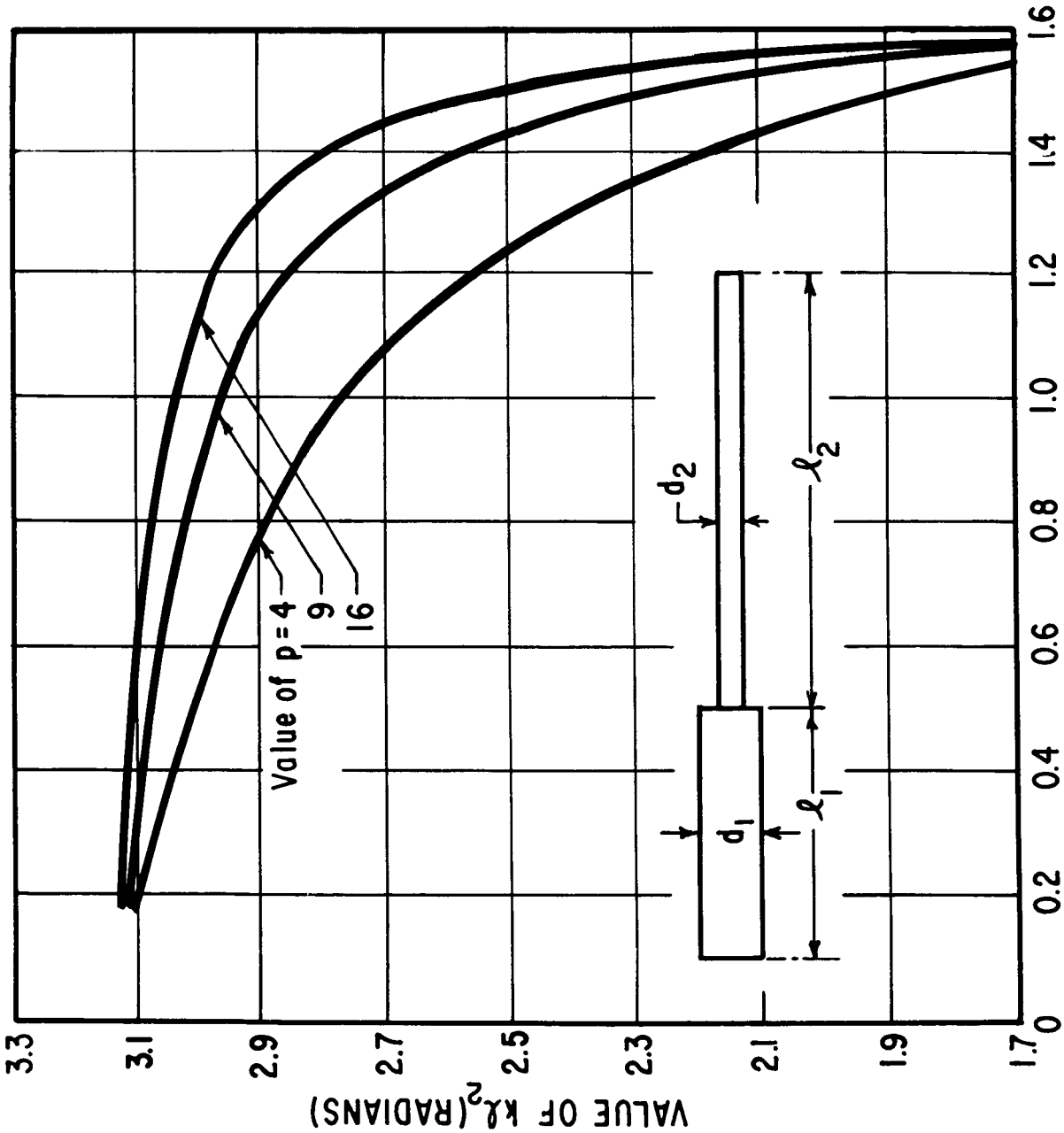

FIGURE 27. DESIGN DIAGRAM FOR FATIGUE SPECIMEN

distance as shown in Figure 28. The slope of this curve gives the strain along the longitudinal axis of the specimen and the maximum strain is directly proportional to the voltage developed in a pick up coil located above the fatigue specimen as shown in Figure 29. Figure 30 shows the relationship between the measured value of the strain, and the calculated value (the calculation being made on the assumption that a pure sine wave travels along a uniform rod). The measured value is about 0.87 times the calculated value because of the distortion of the wave due to the taper. There are a few limitations to this calibration:

1. Reproducibility of specimen geometry and control of surface roughness while machining.

2. Effect of high temperature environment in the case of sodium experiments. Attempts are being made to overcome this limitation.

Using the techniques described above, a series of 1020 mild steel specimens was vibrated in liquid sodium at 300°F. Each point (■) plotted in Figure 31 represents the fatigue failure of a single specimen at a given stress after the elapse of the corresponding number of cycles of alternate stressing. Data for mild steel in distilled water using the same method is included for additional information. Figure 32 shows the failure of a typical specimen in sodium.

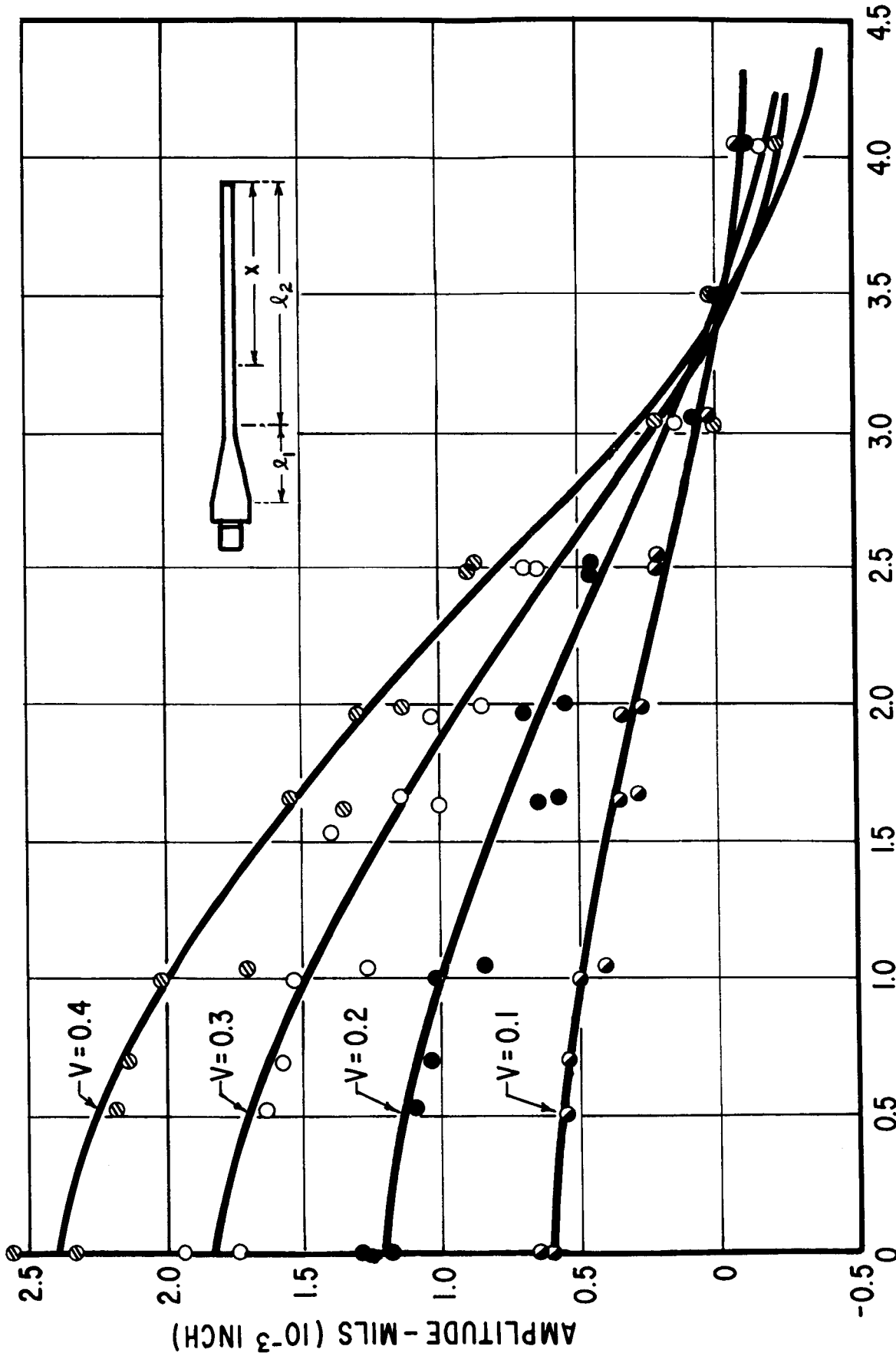

FIGURE 28. CALIBRATION OF FATIGUE SPECIMENS

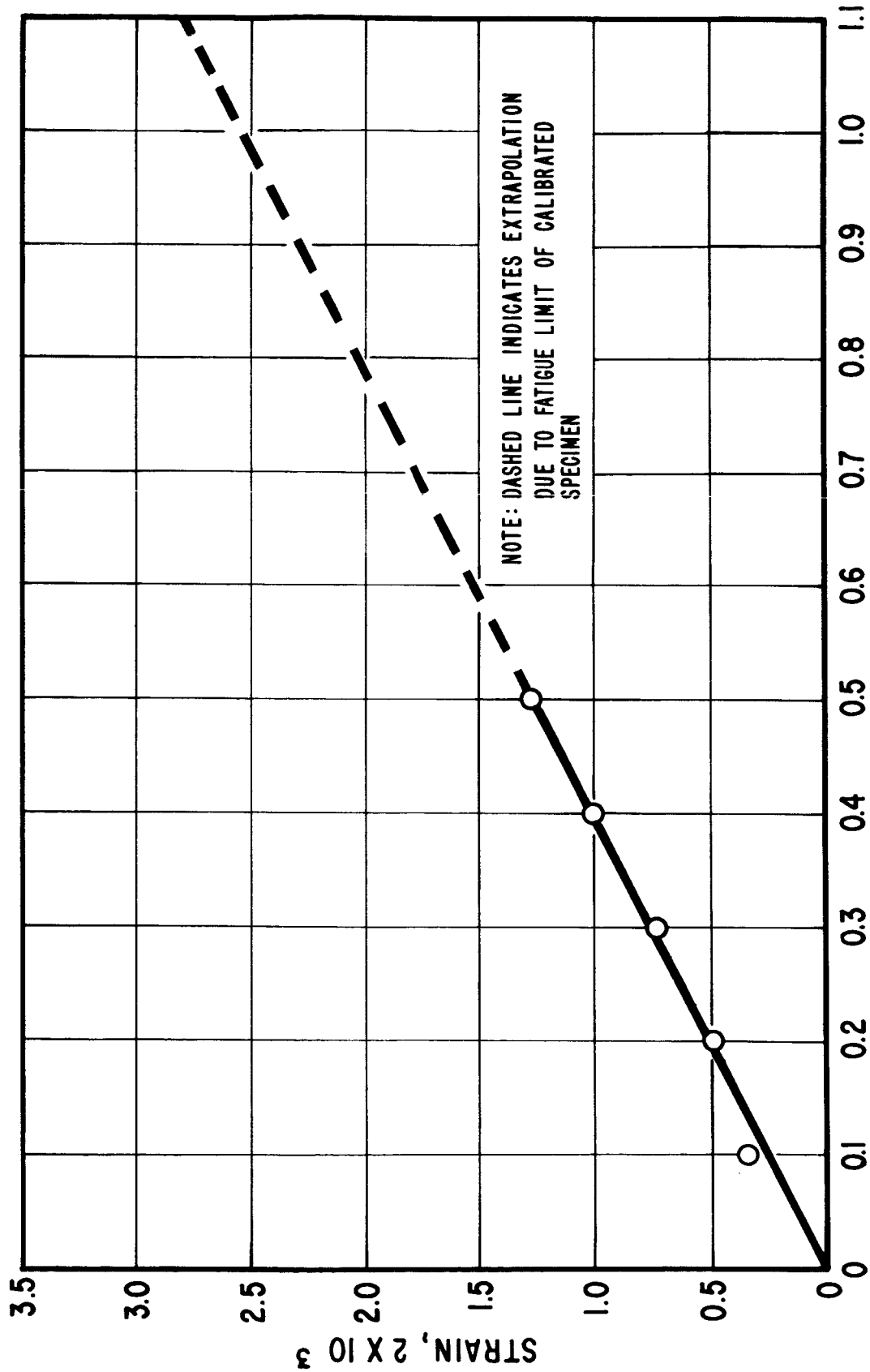

FIGURE 29. CALIBRATION OF FATIGUE SPECIMEN

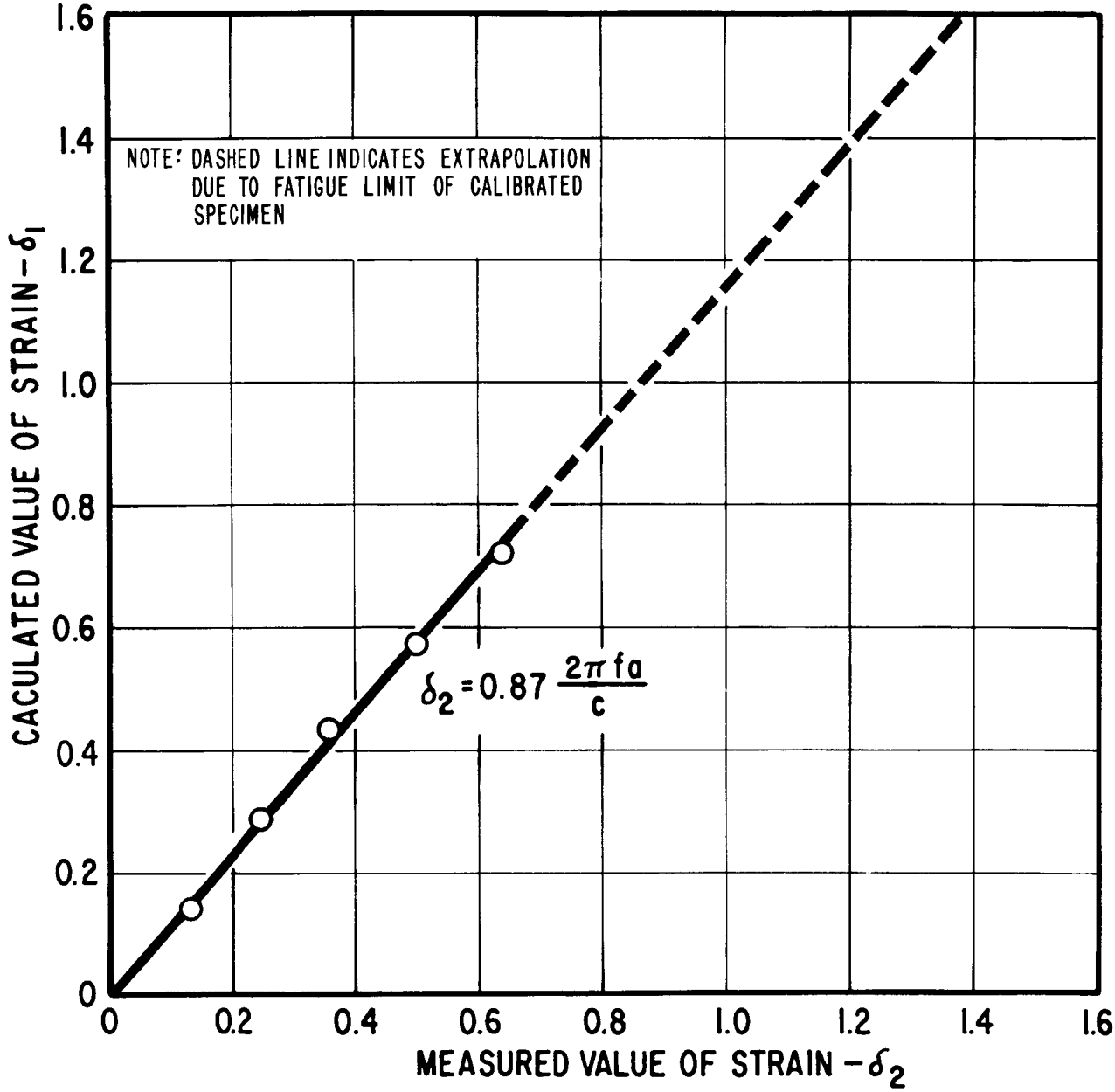

FIGURE 30. CALIBRATION OF HIGH FREQUENCY FATIGUE SPECIMEN

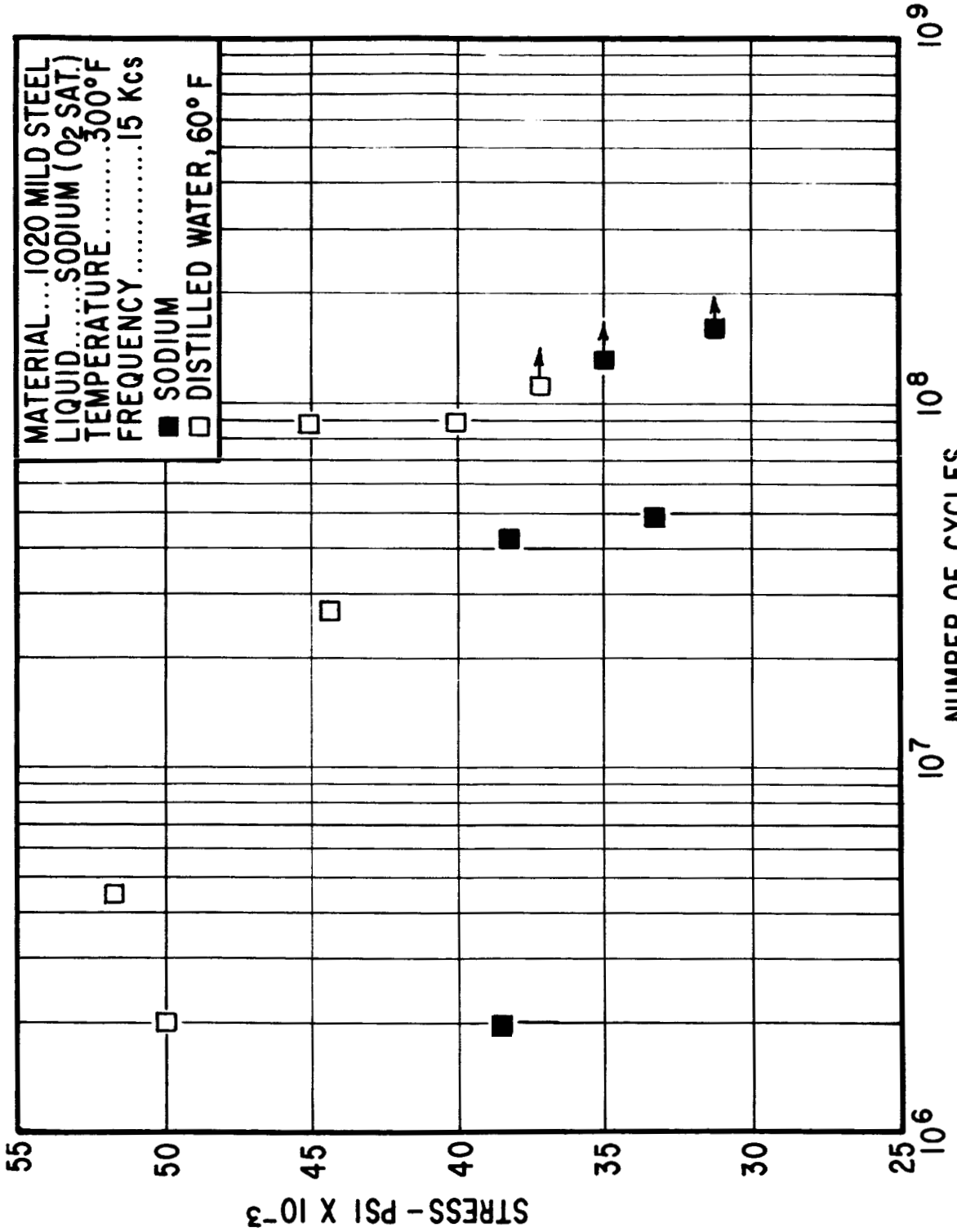

FIGURE 31. HIGH FREQUENCY CORROSION FATIGUE TESTS

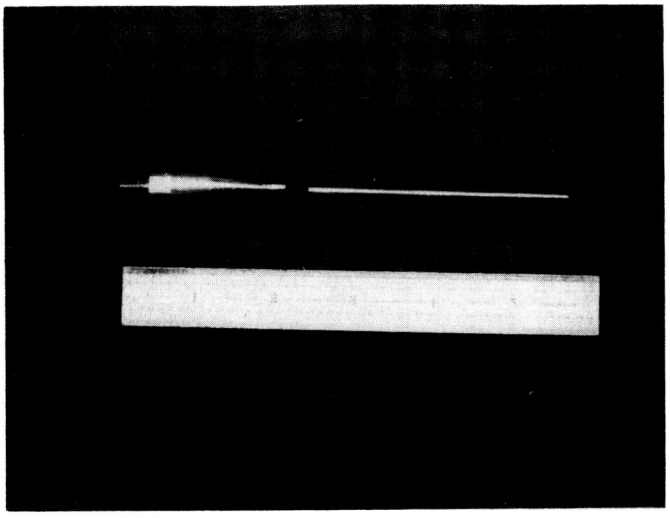

FIGURE 32. TYPICAL FATIGUE SPECIMEN SHOWING FAILURE IN HIGH FEQUENCY TEST

(a) 316 stainless steel (for comparison), (b) TZM, (c) Stellite 6B, (d) Cb-132M, and (e) T-222. The effects of temperature up to 1500°F and oxygen at 10 ± 10 and 200 ● 50 ppm on the cavitation rate in liquid sodium will be studied. Ultrasonic corrosion fatigue and stress corrosion cracking tests in liquid sodium will be performed for 316 and TZM at two temperatures, 1000° and 1500°F, and at the two oxygen levels as above. This work will also be supported by the National Aeronautics and Space Administration under Contract NAS3-4172.

CONCLUSIONS

The results of cavitation damage tests conducted with a magnetostrictive device may be summarized as follows:

1. The rate of cavitation damage in the steady state zone for liquid metal sodium varies as the second power of the displacement amplitude and this result also conforms with that obtained earlier for water systems.

3. The rate of cavitation damage in the steady state zone for liquid sodium increases with temperature and then decreases. Further investigations are necessary to understand the interacting influence of the change in the properties of liquids and test materials as the temperature is increased.

4. Allowing for the lack of accurate information, there is a good correlation between the strain energy of the test material and cavitation damage resistance.

5. The intensity of cavitation damage in liquid sodium at $400^{\circ}F$ is about one and one half times that in water at $80^{\circ}F$ for a given amplitude and frequency.

FURTHER WORK

Work is planned for the coming year to quantitatively study the cavitation damage resistance of four materials which have shown promise for use in advanced nuclear space electric power systems. The new refractory metals dry box facility will be used in these investigations. The metals of interest are:

APPENDIX I

Experiments to Standardize the Test Parameters of Magnetostriction Apparatus:

The essential test parameters of the magnetostriction apparatus are shown in Figure 33. The nomenclature is as follows:

a - amplitude of vibration of the specimen

f - frequency of oscillation

r - radius of the specimen

d - depth of immersion of the specimen

H - depth of test liquid in the beaker

D - diameter of the beaker

λ - wave length of sound in the liquid.

So far there has never been any systematic analysis of the effect of the above parameters on the rate of cavitation damage except for a few isolated experiments without any specific conclusions. Before undertaking any detailed investigations on the resistance of materials by making use of this apparatus, it is necessary to know the effect of small variations in the above parameters so that proper care will be taken to control them as required. With this objective in view the following experiments were carried out under the present program of research. Tap water and aluminum specimens were used in these experiments as a matter of speed and convenience.

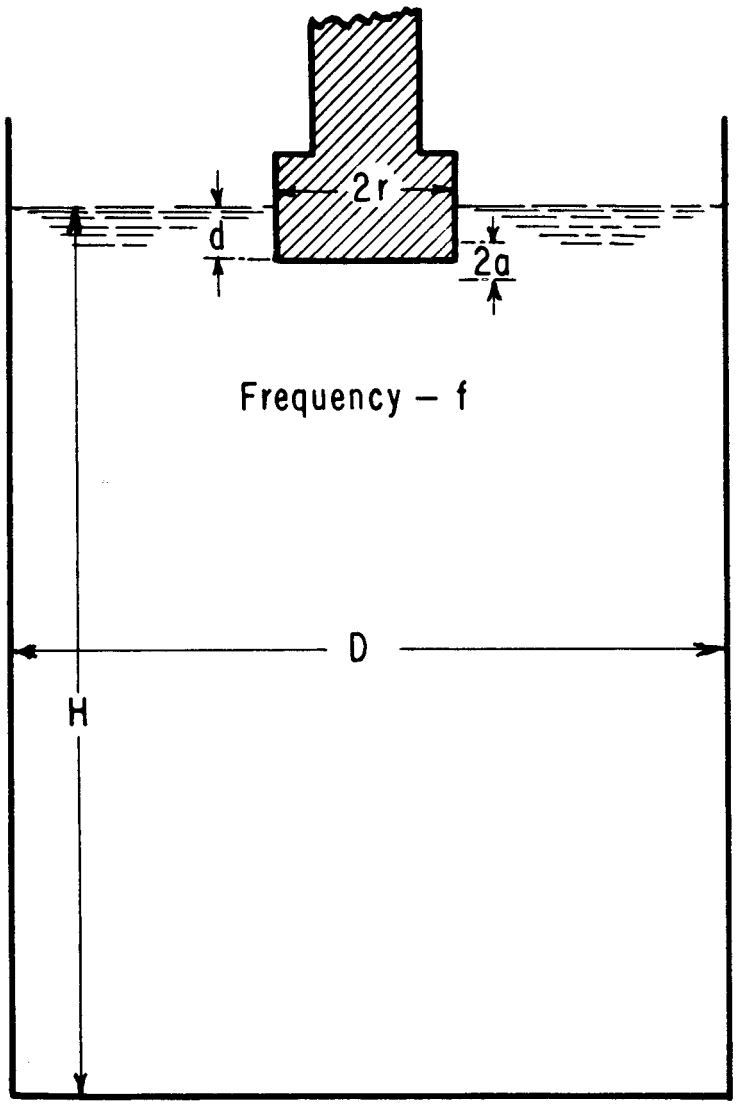

FIGURE 33. DEFINITION SKETCH OF THE MEGNETOSTRICTRICTION APPARATUS

Effect of Specimen Shape: It is the general practice to use a circular test specimen with a flat test face (shown in Figure 34) for cavitation damage tests. However, Plesset (6) reported that it was difficult to get reproducible results with this flat faced specimen and introduced the "dished" specimen idea (as shown in Figure 34) with the claim that this type of specimen would give a better reproducibility of the results. During the present experiments with liquid sodium it was found that the rim damage (the rim of the specimen would break off in the middle of an experiment due to the damage produced by a ring of bubbles entrapped in the tip vortices) was a serious difficulty with this type of specimen. Furthermore, the machining and control of the test surface finish are much more difficult than with the flat faced specimens. These considerations lead to a reexamination of the effect of specimen shape with particular reference to the necessity of the rim. Figure 35 shows the relationship between the damage rate and the testing time for four identical flat faced specimens at a given amplitude and frequency. Figure 36 shows the same relationship for three identical, Plesset, dished specimens. The amplitude in this case had to be lower because of rim damage at higher amplitudes. One can easily see that the reproducibility of results with a flat faced specimen is in no way inferior to the specimens with rim. Figure 37 shows the rate of damage as a function of amplitude for both types in the steady zone and there seems to be no difference provided there is no rim damage. It has been decided to adopt a simple flat faced specimen as a result of these investigations.

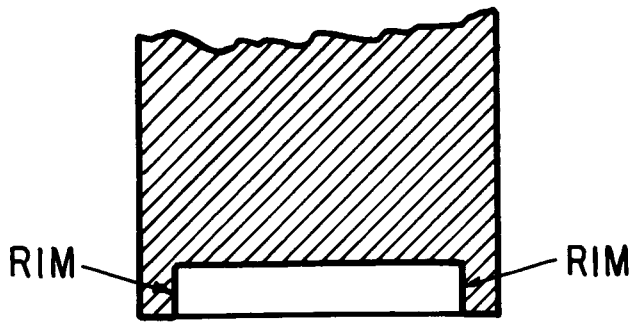

a) PLESSET'S RIMMED SPECIMEN

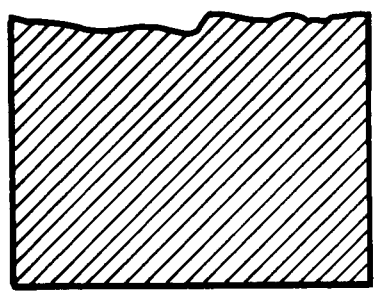

b) FLAT SPECIMEN

FIGURE 34. TWO TYPES OF SPECIMENS TESTED FOR REPRODUCIBILITY

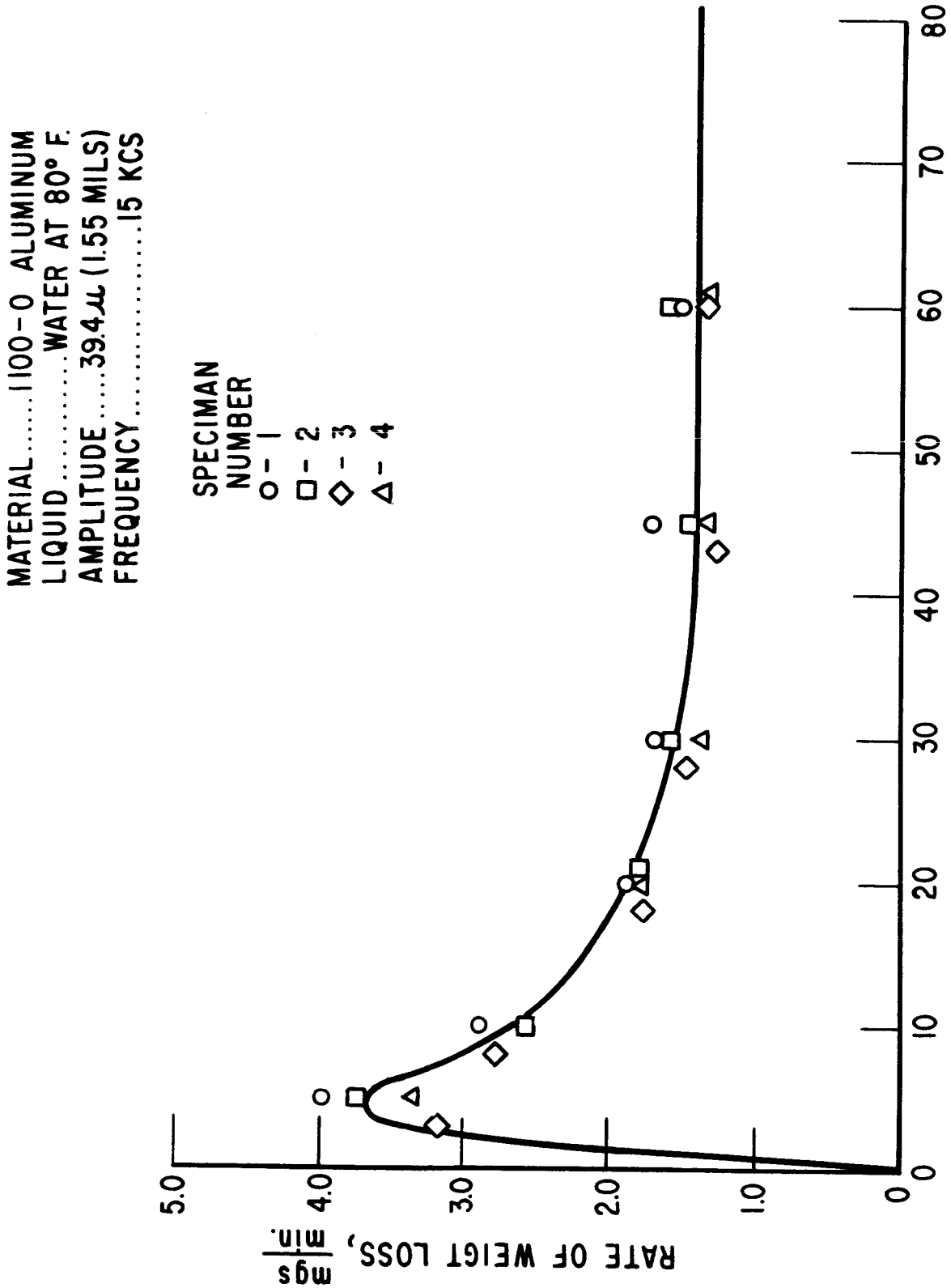

FIGURE 35. SHOWING REPRODUCIBILITY WITH FLAT-FACED SPECIMEN

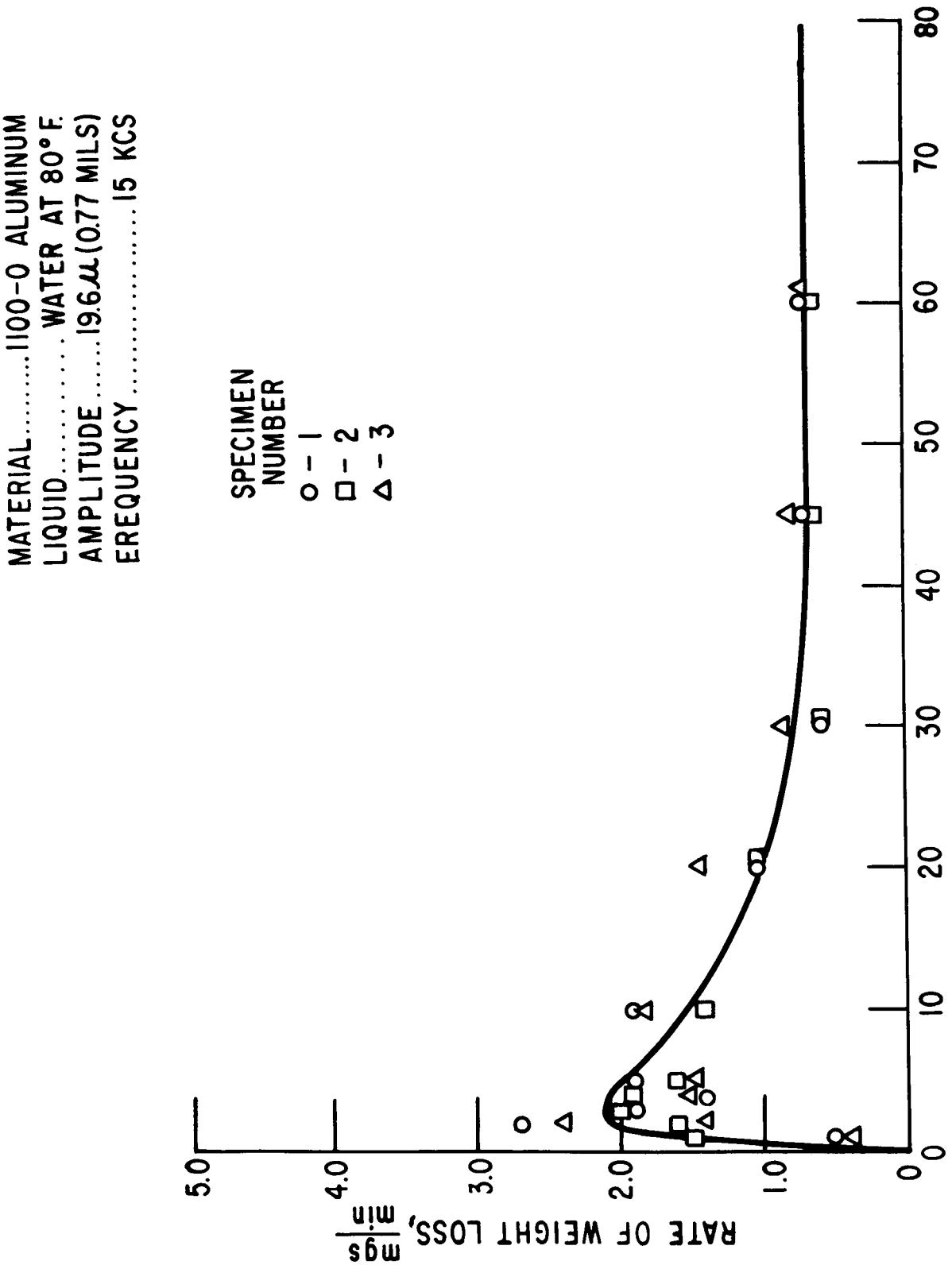

FIGURE 36. SHOWING REPRODUCIBILITY WITH PLESSET'S RIMMED SPECIMAN

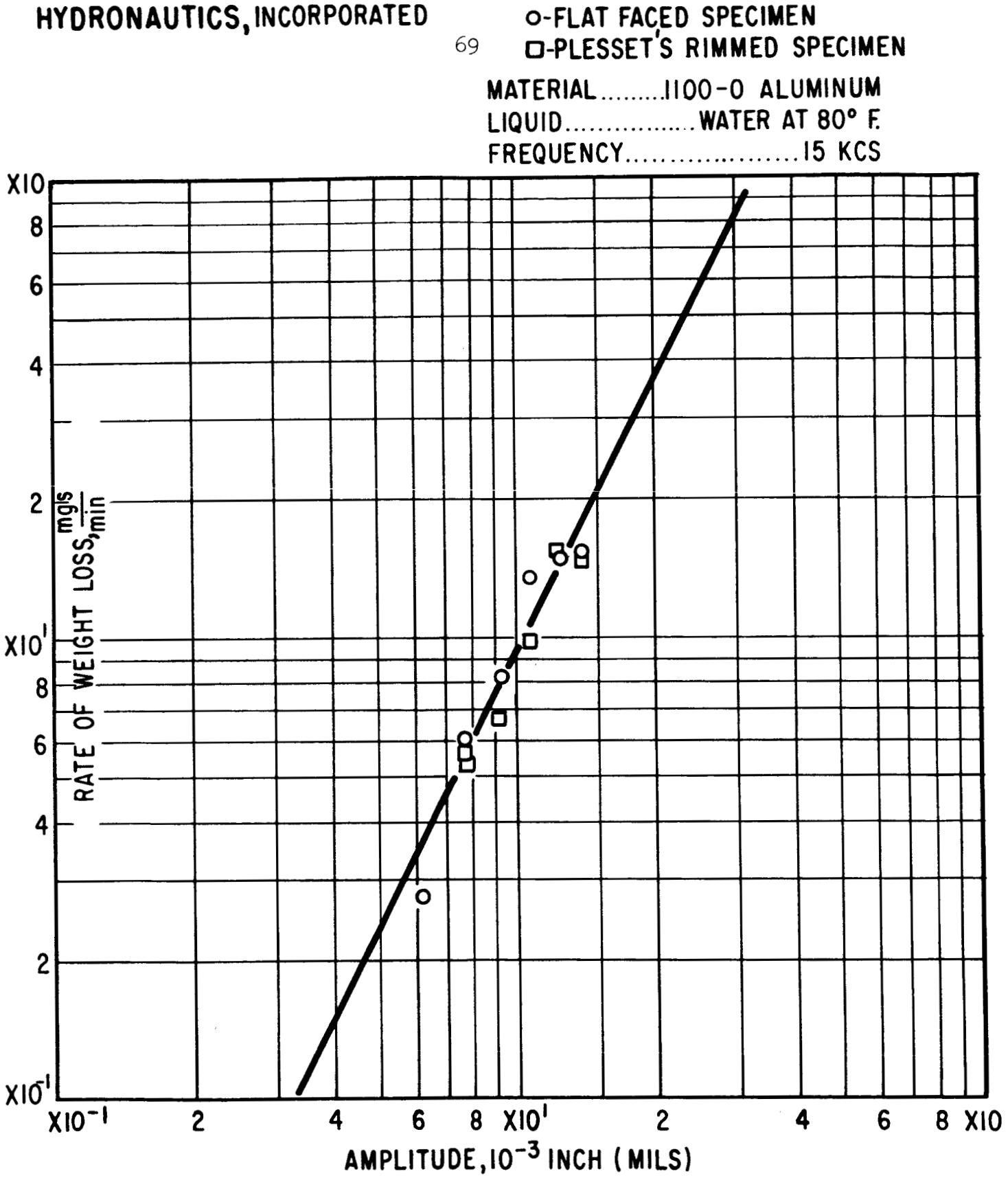

FIGURE 37. EFFECT OF AMPLITUDE ON RATE OF WEIGHT LOSS FOR BOTH TYPES OF SPECIMENS

Effect of Depth of Test Liquid in the Beaker: It has been suggested earlier that the depth of liquid in the beaker had an effect on the damage rate because of the wave reflections in the liquid (23). It has been further recommended that this depth should be a half wave length of sound in that liquid for the test frequency so that a standing wave is produced. Figure 38 shows the relationship between the rate of damage and the relative depth of liquid (water) with respect to the wave length at 15 kcs. There seems to be little effect on damage rate due to the wave reflections up to about two and one half wave lengths. It has been observed that the damage rate decreases if the depth is decreased below 0.3 wave length. Hence the depth of liquid in the beaker will be kept more than a half wave length.

Effect of the Diameter of the Beaker: There seems to be little effect of the diameter of the beaker on the rate of damage as shown in Figure 39 which shows the relationship between the rate of damage and the relative diameter with respect to the wave length of sound in the test liquid.

Effect of Depth of Immersion of Specimen: Rheingans (13) found that the depth of immersion of the test specimen had an effect on the cumulative damage; furthermore, this effect depended upon the test duration. Because of the two interacting variables, he failed to come to a definite conclusion regarding the magnitude of the effect of the depth of immersion on damage. Present experiments on this aspect conducted in the steady zone (thereby eliminating the time effects) show that the rate of

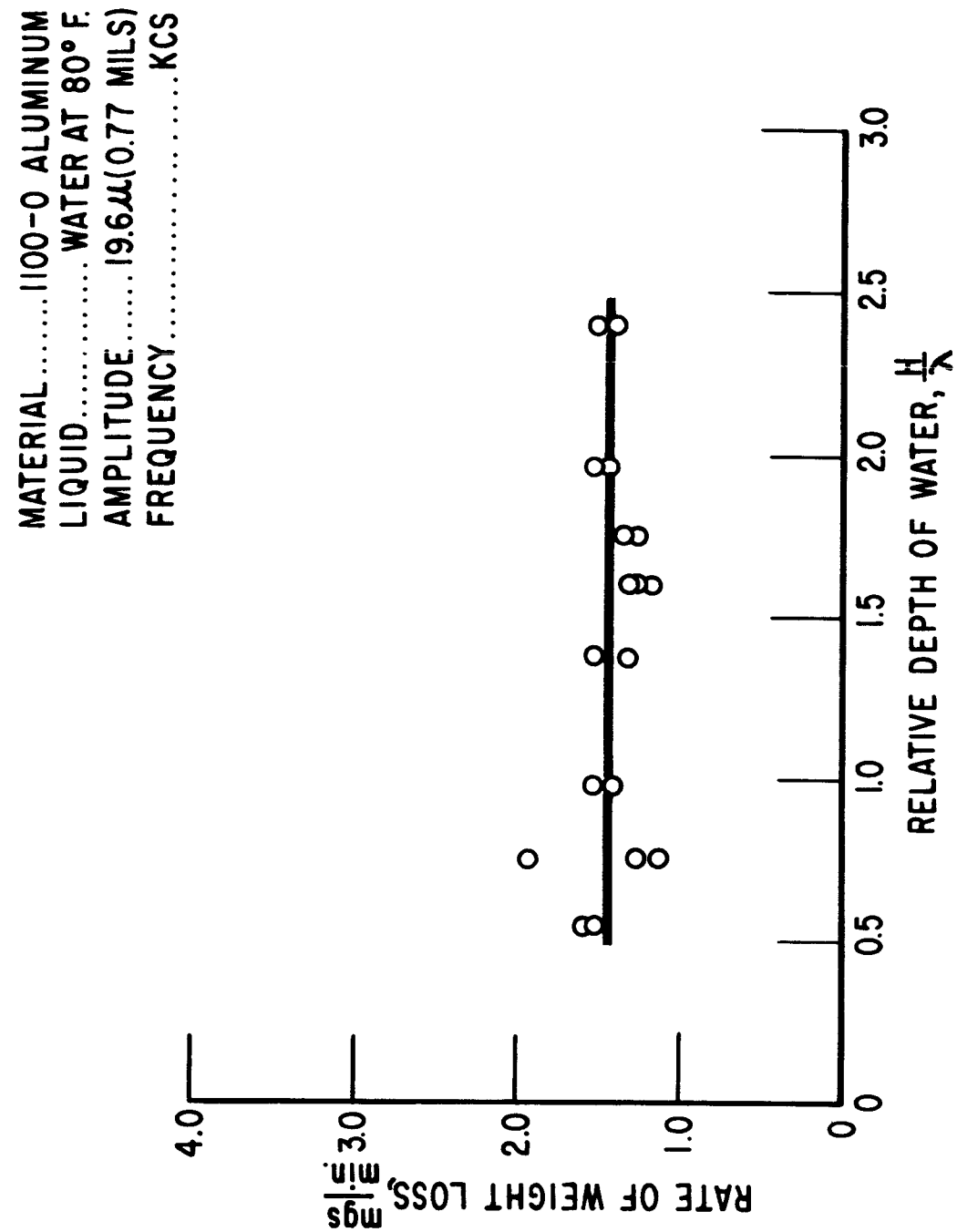

FIGURE 38. EFFECT OF DEPTH OF LIQUID IN THE BEAKER ON RATE OF WEIGHT LOSS

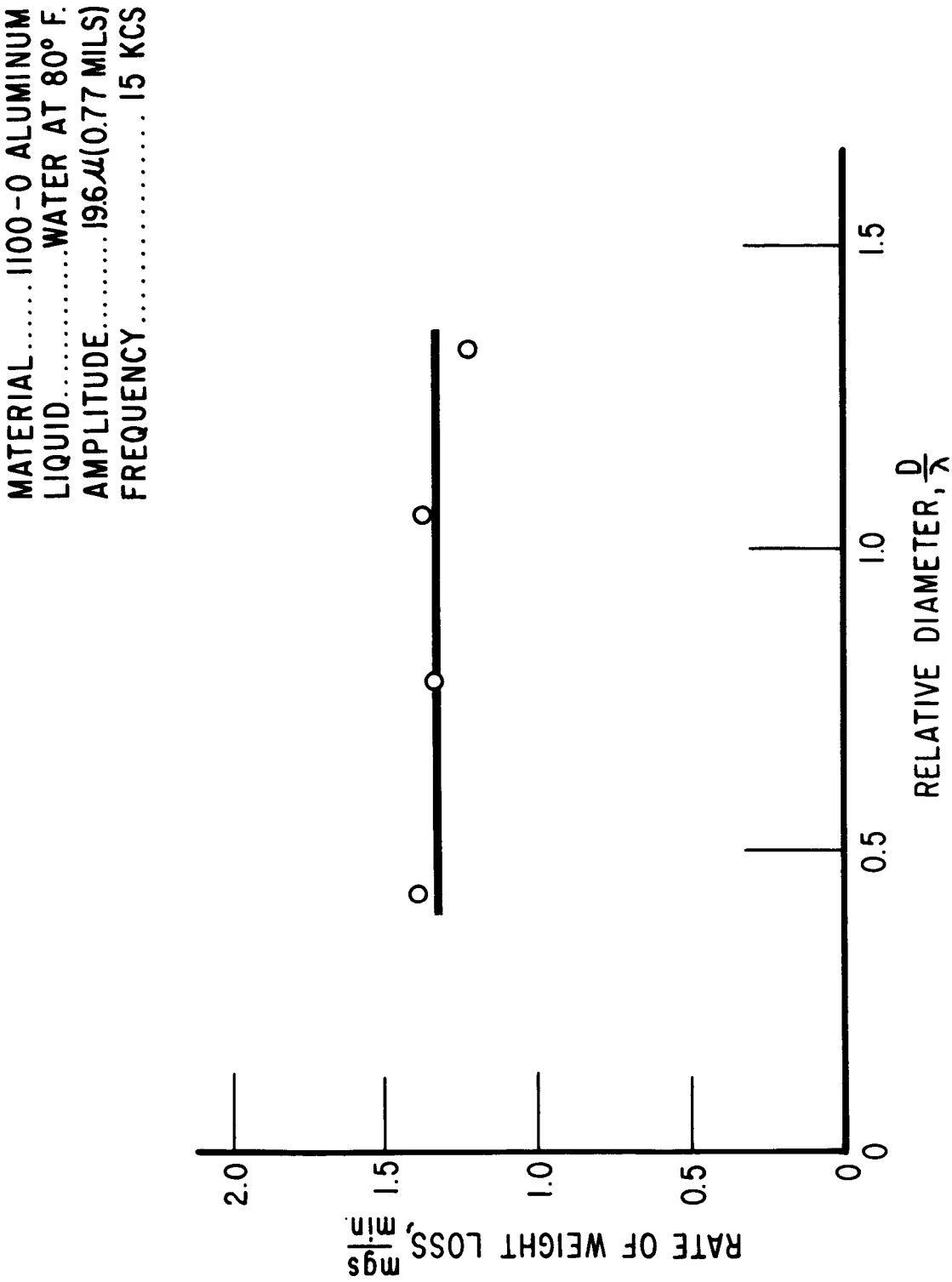

FIGURE 39. EFFECT OF BEAKER DIAMETER ON RATE OF WEIGHT LOSS

damage in the steady zone is independent of the depth of immersion of the test specimen up to one radius of the specimen as shown in Figure 40.

Effect of Diameter of Specimen: The rate of weight loss due to cavitation damage in the steady state zone at a given amplitude and frequency is directly proportional to the square of the diameter of the specimen within the limits of 3/8 to 7/8 inch diameter for flat specimens as shown in Figure 41. The rate of volume loss is determined by the area of specimen and this value was found to be independent of the specimen diameter as shown in Figure 42. This result leads to the interesting conclusion that the intensity of cavitation damage is independent of the specimen diameter, within the range tested, in the case of a magnetostriction apparatus in the steady state zone (the intensity being defined as in Reference (9)).

Conclusions: As a result of these analyses, the following criteria for standardization of the test parameters in the magnetostriction apparatus have been formulated. The beaker dimensions do not seem to have any specific effect on the rate of damage and hence a reasonably practical size may be selected. The rate of damage is independent of the depth of immersion of the specimen up to one radius of the specimen. A flat faced specimen may be selected for testing because of its simplicity.

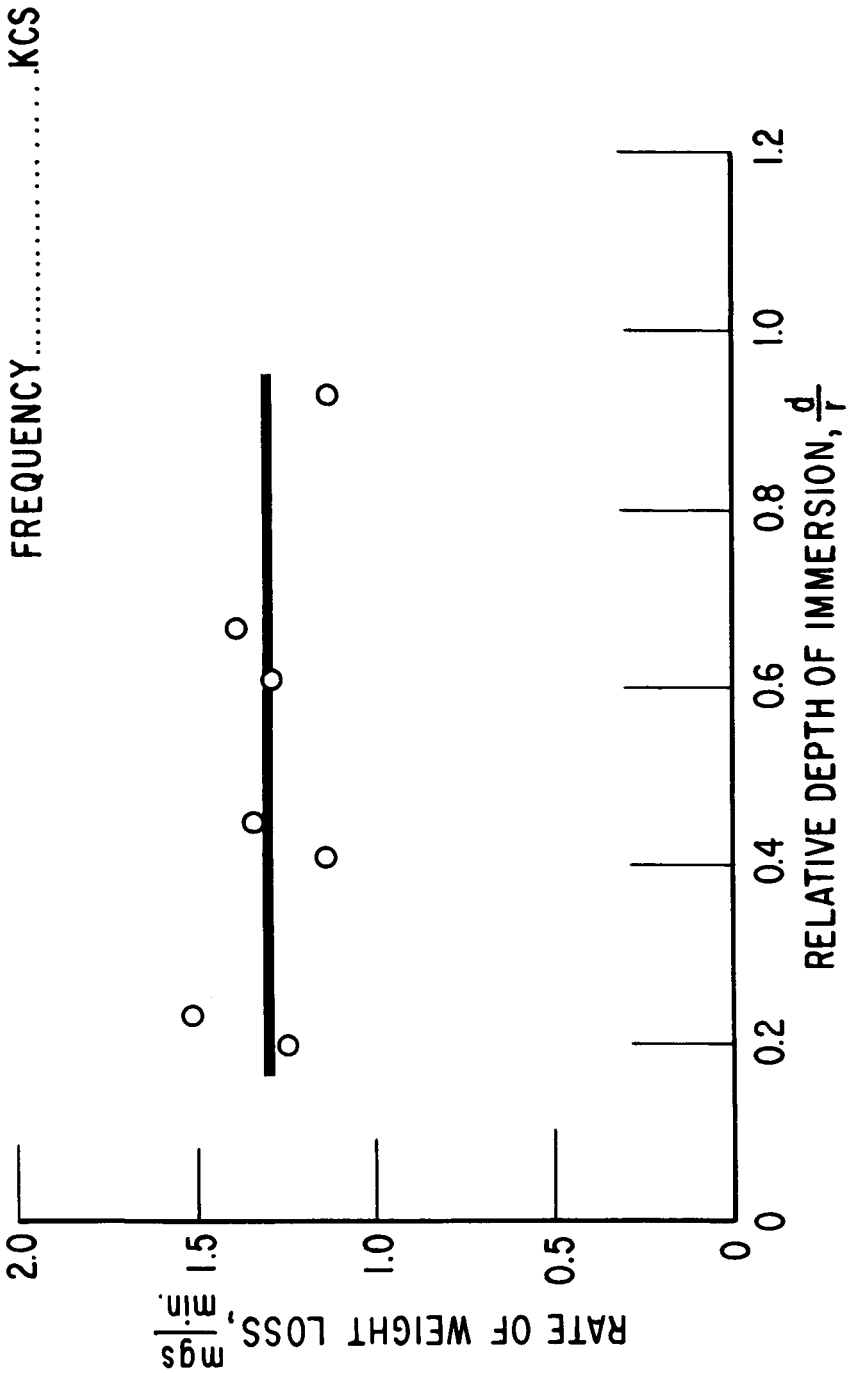

FIGURE 40. EFFECT OF DEPTH OF IMMERSION OF SPECIMAN ON RATE OF WEIGHT LOSS

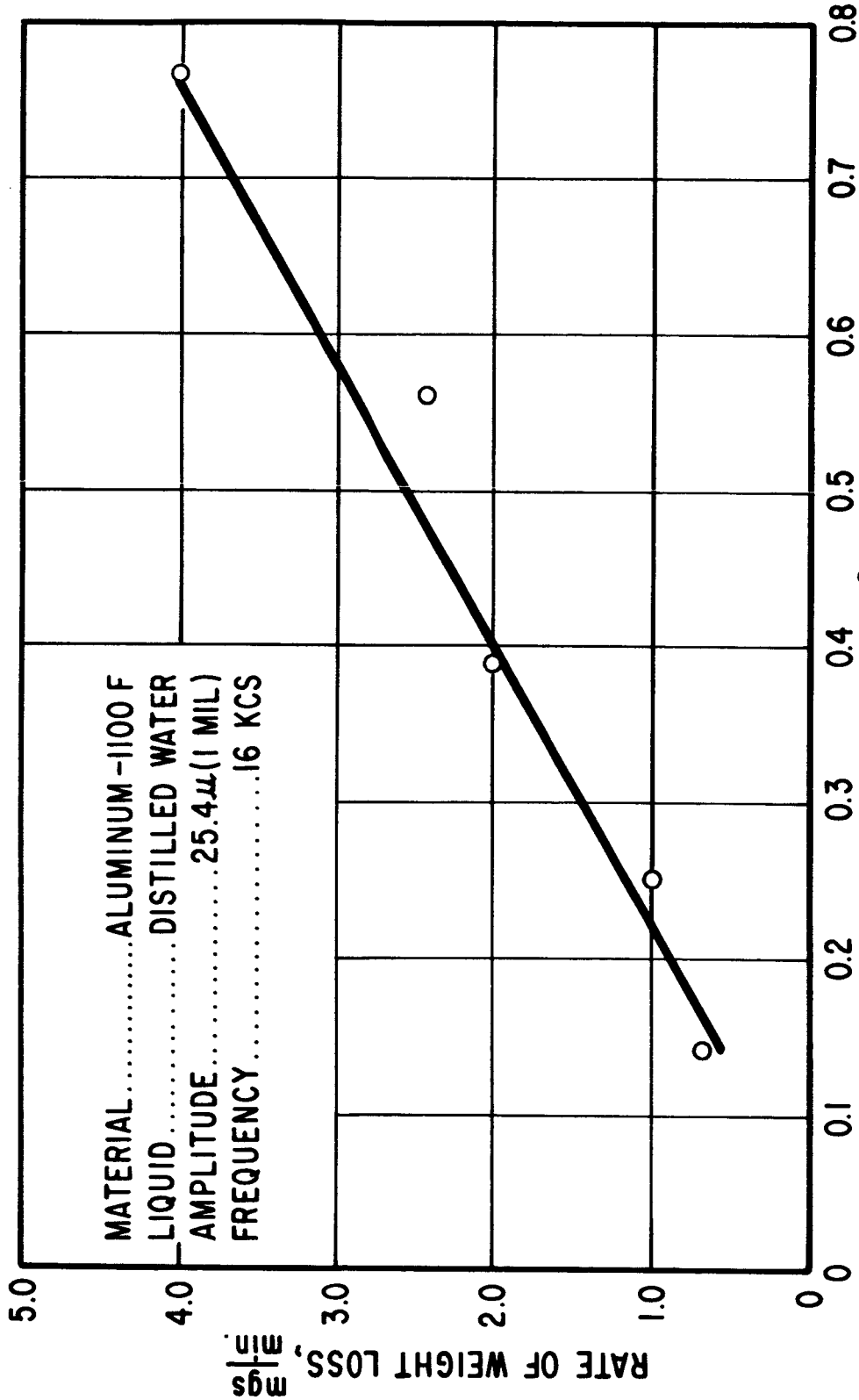

FIGURE 41. EFFECT OF SPECIMEN DIAMETER^2 ON RATE OF WEIGHT LOSS

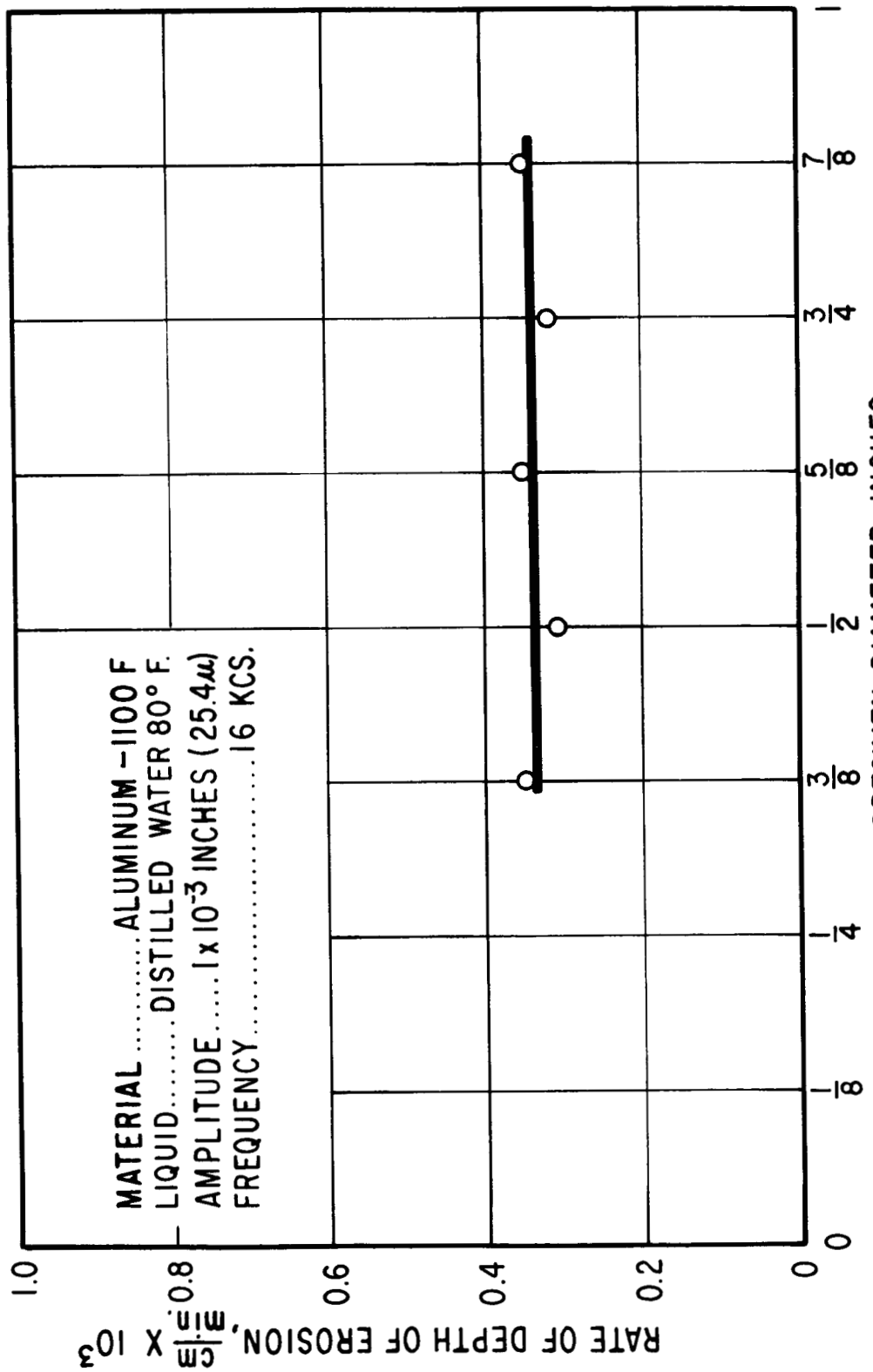

FIGURE 42. EFFECT OF SPECIMEN DIAMETER ON RATE OF AVERAGE DEPTH OF EROSION

APPENDIX II

The Design and Function of the Components of the Magnetostriction Apparatus

Description

Refer to the block diagram in Figure 3. Basically the system consists of a nickel transducer element which contracts in length under the influence of a magnetic field. This is known as the magnetostrictive effect. The magnetic coil surrounding the stack is powered by an oscillating current source which causes the stack to vibrate longitudinally in phase with the oscillation cycle. The amplitude of vibration of the nickel transducer is limited by its magnetization characteristics and modulus of elasticity and is usually quite small, even at resonance. In order to further amplify this vibratory motion to useful output levels it is necessary to mechanically couple a velocity transformer to the working end of the transducer. In the work reported, an exponential horn or a double cylinder stepped horn is used. Careful impedance matching of the electromechanical coupling of the transducer and transformer elements is essential for efficient operation. The technique of design is described in detail in the literature (7), (24), (25).

Equipment Details

The particular apparatus used in these investigations are as follows:

Transducer - A commercial transducer was used which consisted of a pure laminated nickel stack made up of annealed U shaped sheets of pure nickel about 0.005 inch thick. Each lamination was coated with an epoxy resin and potted together to form a ridged rectangular assembly, having a cross section of 1-3/4" x 2" and a length of 6 inches. A pair of insulated exciting coils, wound in a series aiding direction is fitted over each leg of the slotted transducer. The resonant frequency of the transducer is 14 kcs. The power requirements are about 200 watts to produce an amplitude at the transducer of about 0.0005 inch. The impedance of the transducer uncoupled is about 16 ohms. DC biasing is furnished by means of a permanent magnet positioned in the open end of the slot.

Velocity Transformer - A threaded stub is firmly attached to the transducer by means of soldering so that an interchangeable velocity transformer can be adapted. For cavitation damage work, the exponential horn is used, and for fatigue studies the higher amplitude double cylinder horn is used. The amplification factor for an exponential horn varies directly as the ratio of the larger and smaller diameters. For the double cylindrical horn greater amplifications can be realized, because the amplification factor varies as the ratio of the square of the larger and smaller diameters. In actual practice, it turns out that the double cylinder horn is extremely sensitive to impedance matching and therefore great care must be taken to insure proper electro-mechanical coupling in order to obtain the full amplification capability. However, for the purposes of

these experiments, fairly good results have been obtained using a general purpose fixed transducer design. The materials of construction for velocity horns have been 17-7PH stainless steel, 316 stainless steel and titanium, 6Al, 4V alloy.

Cooling - The heat generated in the exciting coils of the transducer plus the vibrational energy transmitted by the magnetostrictive effect must be dispelled in order not to alter the operating constants of the equipment. Successful cooling has been obtained by submerging the unit in a kerosene bath containing a cooling water coil.

Amplifier - Any standard linear amplifier (push-pull type) can be used by powering the transducer exciting coils.

Audio Oscillator - The amplifier is driven by a standard audio oscillator capable of stable frequency control over a range of 20 kcs. A wide range gain control for regulating the input signal is required. The oscillating input to the amplifier imparts an oscillating current to the exciting coils causing the transducer to be driven in a vibratory mode of the same frequency. Turning of the oscillator to the resonant frequency of the system will produce maximum amplitude.

Pick-up Coil - Some means of measuring the amplitude of vibration is required. Any means is satisfactory in generating an electrical signal as a function of physical displacement. Piezoelectric transducers, reluctance and capacitance pick-ups have been used by others with success. The method employed in these investigations is to provide a simple coil of fine wire

(similar to a voice coil of a loudspeaker) at an anti-nodal point on the velocity transformer. The residual magnetic field existing in the velocity transformer is sufficient to generate a voltage signal in the coil which varies with the amplitude. Sometimes when paramagnetic materials are used, the signal output of the coil can be increased by means of a fixed ring magnet mounted in close proximity to the coil. The voltage output of the coil is fed to any standard oscilloscope. The amplitude of the sine wave generated (voltage) is a function of the physical amplitude of the specimen. This signal voltage can be calibrated against the measured physical displacement by means of observations of a fixed point on the specimen through a filar microscope.

REFERENCES

1. Hammitt, F. G., "Observations on Cavitation Damage in a Flowing System," Trans. A.S.M.E., Vol. 85, Series D, No. 3, Jour. Basic Engr., pp. 347-359, September 1963.

2. Kelly, R. W., Wood, G. M., Marman, H. V., and Milich, J.J., "Rotating Disk Approach for Cavitation Damage Studies in High Temperature Liquid Metal," A.S.M.E. Paper No. 33-AHGT-26, 1963.

3. "Development of Hermetically Sealed Centrifugal Pump Units for Liquid Metals," Report No. 43-112, Nuclear Power Section, Allis-Chalmers Manufacturing Company, Milwaukee, Wisconsin, June 30, 1953.

4. Eisenberg, Phillip, "Cavitation Damage," HYDRONAUTICS, Incorporated Technical Report 233-1, December 1963.

5. Mason, W. P., "Internal Friction and Fatigue in Metals at Large Strain Amplitudes," Jour. Acoustic Soc. Am., Vol. 28, No. 6, pp. 1207-1218, 1956.

6. Plesset, M. S., "On Cathodic Protection in Cavitation Damage," Trans. A.S.M.E., Vol. 82, Series D, No. 4, Jour. Basic Engr., pp. 808-817, December 1960.

7. Neppiras, E. A., "Very High Energy Ultrasonics," British Jour. of Applied Physics, Vol. 11, pp. 143-150, April 1960.

8. Thiruvengadam, A., and Preiser, H. S., "On Testing Materials for Cavitation Damage Resistance," HYDRONAUTICS, Incorporated Technical Report 233-3, December 1963.

9. Thiruvengadam, A., "A Comparative Evaluation of Cavitation Damage Test Devices," HYDRONAUTICS, Incorporated Technical Report 233-2, November 1963.

10. Nowotny, H., "Destruction of Material Through Cavitation-Investigation with an Oscillator," VDI-Verlag Gimbh Berlin, 1942, English Translation as ORA Report No. 03424-15-I, Nuclear Engineering Department, University of Michigan, 1962.

11. Leith, W. C., and Thompson, A. L., "Some Corrosion Effects in Accelerated Cavitation Damage," Trans. A.S.M.E. Vol. 82, Series D, No. 4, Jour. Basic Engr., pp. 799, December 1960.

12. Plesset, M. S., "Pulsing Technique for Studying Cavitation Erosion of Metals," Corrosion, National Association of Corrosion Engineers, pp. 183-t, December 1960.

13. Rheingans, W. J., "Accelerated-Cavitation Research," Trans. A.S.M.E., Vol. 72, No. 5, pp. 705-719, July 1950.

14. Thiruvengadam, A., "A Unified Theory of Cavitation Damage," Trans. A.S.M.E., Vol. 85, Series D, No. 3, Jour. Basic Engr., pp. 365-376, September 1963.

15. Hammitt, et. al., "Cavitation Damage in Mercury and Water in a Cavitating Venturi and Other Components," Technical Report No. 9, College of Engineering, Department of Nuclear Engineering, Laboratory for Fluid Flow and Heat Transport Phenomena, September 1963.

16. Morrow, JoDean, "An Investigation of Plastic Strain Energy as a Criterion for Finite Fatigue Life," The Garrett Corporation, Phoenix, Arizona, August 1960.

17. "Steels for Elevated Temperature Service," United States Steel, Fourth Printing, 1961.

18. Thompson, J. G., "Nickel and Its Alloys," National Bureau of Standards Circular 592, U. S. Department of Commerce, pp. 25, February 1958.

19. "Engineering Properties of Inconel Alloy 600," Technical Bulletin T-7, Huntington Alloy Products Division, The International Nickel Company, Inc., 1961.

20. Taylor, L., editor, "Metals Handbook," American Society for Metals, pp. 432, 1948.

21. Neppiras, E. A., "Techniques and Equipment for Fatigue Testing at Very High Frequencies," Proc. ASTM, Vol. 59, 1959.

22. Tanaka, S., "Ultrasonic Fatigue Testing," Rep. Inst. High Sp. Mech., Japan, Vol. 13, No. 129, 1961/1962.

23. Robinson, L. E., Holmes, B. A., and Leith, W. C., Progress Report on Standardization of the Vibratory-Cavitation Test, Trans. A.S.M.E. Vol. 80, pp. 103-107, 1958.

24. Wise, B. A., "Design of Nickel Magnetostriction Transducers," Platinum Metals and Applied Physics Section, Development and Research Division, The International Nickel Company, Inc.

25. Hueter, T. F., Bolt, R. H., "Sonics," John Wiley and Sons, Inc., New York, London, Third Printing, June 1962.

DISTRIBUTION LIST
(Contract NASr- 105)

Mr. Herbert D. Rochen (Snap 50/SPub)
NASA-AEC Deputy
Atomic Energy Commission
Washington 25, D. C. 1

NASA-Ames Research Center
Moffett Field, California, 94035
Attn: Library 1

NASA - Langley Research Center
Langley Station
Hampton, Virginia, 23365
Attn: Library 1

NASA - Lewis Research Center
21000 Brookpark Road
Cleveland, Ohio, 44135
Attn: J. J. Fackler (86-1) 1
Dr. B. Lubarsky (86-1) 1
R. F. Mather (86-5) 1
J. P. Couch (86-5) 1
M. J. Hartmann (5-9) 1
C. H. Hauser (5-9) 1
S. G. Young (49-1) 1
Library 1
Office of Reliability and Quality Assurance 1
Patent Counsel 1

NASA - Marshall Space Flight Center
Huntsville, Alabama, 35812
Attn: Library 1

NASA - Scientific and Technical Information Facility
Box 5700
Bethesda 14, Maryland
Attn: NASA Representative 2

Jet Propulsion Laboratory
4800 Oak Grove Drive
Pasadena, California, 91103
Attn: Library 1

Brookhaven National Laboratory
Upton, Long Island, New York
Attn: Dr. O. E. Dwyer 1

U. S. Atomic Energy Commission
Division of Technical Information Extension
P. O. Box 62
Oak Ridge, Tennessee 2

Defense Documentation Center
Cameron Station
Alexandria, Virginia 2

United Aircraft Corporation
Pratt and Whitney Aircraft Division, CANEL
P. O. Box 611
Middletown, Connecticut
Attn: G. M. Wood 1

University of Michigan
Dept. of Nuclear Engineering
North Campus
Ann Arbor, Michigan
Attn: Dr. F. G. Hammitt 1

National Aeronautics and Space Administration
J. J. Lynch, Code RNP
1512 H. Street, N. W.,
Washington, D. C. 20546 1

General Electric Company
Space Division
Space, Power and Propulsion Section
Cincinnati, Ohio, 45215
Attn: Dr. J. W. Semmel 1
Mr. E. Schnetzer 1

Chief, Bureau of Ships (634A)
Navy Department
Washington 25, D. C.
Attn: Mr. L. S. Birnbaum 1

Deputy Chief of Staff Research and Development
Department of Defense
Washington 25, D. C. 1

Chief of Staff, U. S. Army
Physical Sciences Division
Washington 25, D. C. 1

Office of the Chief of Engineers
Department of the Army
Nuclear Power Division
Washington 25, D. C. 1

Office of the Chief of Ordnance
Department of Army
Research and Development Division
Washington 25, D. C. 1

Office of Chief of the Signal Corps
Department of the Army
Research and Development Division
Missile and Space Office
Washington 25, D. C. 1

Office of Naval Research
Material Sciences Division
Washington 25, D. C. 1

Office of Chief of Naval Operations
Department of Navy
Fleet Ballistic Missiles Division
Washington 25, D. C. 1

Office of Chief,
Research and Development
Maritime Administration
Washington 25, D. C.
Attn: E. McCutcheon 1

Chief, Bureau of Naval Weapons
Astronautics Division
Washington 25, D. C. 1

Chief, Bureau of Ships
Applied Science Branch
Washington 25, D. C.
Attn: E. Bukzin 1

W. J. Rheingans
Assistant General Manager
Allis Chalmers Manufacturing Company
York, Pennsylvania 1

Office of Naval Research
Mechanics Branch
Washington 25, D. C.
Attn: S. Doroff 1

J. Lichtman
Material Sciences Division
U. S. Naval Applied Science Laboratory
Naval Base
Brooklyn 1, New York 1

W. L. Miller
Physical Sciences Division
U. S. Naval Applied Science
Laboratory
Naval Base
Brooklyn 1, New York 1

Dr. A. T. Ellis
Department of Applied Mechanics
California Institute of Technology
Pasadena, California 1

Dr. M. S. Plesset
Department of Applied Mechanics
California Institute of Technology
Pasadena, California 1

Dr. John P. Craven, Chief Scientist
Special Projects Office
Bureau of Naval Weapons
Department of the Navy
Washington 25, D. C.